J Bioenerg Biomembr (2011) 43:541–564
DOI 10.1007/s10863-011-9381-4

HYPOTHESIS

Mammalian NADH:ubiquinone oxidoreductase (Complex I) and nicotinamide nucleotide transhydrogenase (Nnt) together regulate the mitochondrial production of H_2O_2—Implications for their role in disease, especially cancer

Simon P. J. Albracht · Alfred J. Meijer · Jan Rydström

Received: 14 June 2011 / Accepted: 3 August 2011 / Published online: 1 September 2011

Abstract Mammalian NADH:ubiquinone oxidoreductase (Complex I) in the mitochondrial inner membrane catalyzes the oxidation of NADH in the matrix. Excess NADH reduces nine of the ten prosthetic groups of the enzyme in bovine-heart submitochondrial particles with a rate of at least 3,300 s^{-1}. This results in an overall NADH→O_2 rate of ca. 150 s^{-1}. It has long been known that the bovine enzyme also has a specific reaction site for NADPH. At neutral pH excess NADPH reduces only three to four of the prosthetic groups in Complex I with a rate of 40 s^{-1} at 22 °C. The reducing equivalents remain essentially locked in the enzyme because the overall NADPH→O_2 rate (1.4 s^{-1}) is negligible. The physiological significance of the reaction with NADPH is still unclear. A number of recent developments has revived our thinking about this enigma. We hypothesize that Complex I and the Δp-driven nicotinamide nucleotide transhydrogenase (Nnt) co-operate in an energy-dependent attenuation of the hydrogen-peroxide generation by Complex I. This co-operation is thought to be mediated by the NADPH/$NADP^+$ ratio in the vicinity of the NADPH site of Complex I. It is proposed that the specific H_2O_2 production by Complex I, and the attenuation of it, is of importance for apoptosis, autophagy and the survival mechanism of a number of cancers. Verification of this hypothesis may contribute to a better understanding of the regulation of these processes.

Keywords NADH:ubiquinone oxidoreductase · Transhydrogenase · Reactive oxygen species (ROS) · Cancer

Abbreviations

Ech	*Escherichia coli* hydrogenase-3-type hydrogenase from *Methanosarcina barkeri*
EM	Electron microscopy
EPR	Electron paramagnetic resonance
Fe-S	Iron sulphur
HIF	Hypoxia-inducible transcription factor
IRE	Iron-response element
Nnt	Δp-driven nicotinamide nucleotide transhydrogenase
PDH	Pyruvate dehydrogenase
PDK	Pyruvate dehydrogenase kinase
ROS	Reactive oxygen species
SMP	Submitochondrial particles
SOD	Superoxide dismutase
TTFA	2-thenoyl-trifluoroacetone
UCP2	Uncoupling protein 2
Δp	Protonmotive force
$\Delta\Psi_m$	Mitochondrial membrane potential.

S. P. J. Albracht (✉)
Swammerdam Institute for Life Sciences,
University of Amsterdam,
Science Park 904 (Room C3.272),
NL-1098 XH Amsterdam, The Netherlands
e-mail: s.p.j.albracht@uva.nl

A. J. Meijer
Department of Medical Biochemistry, Academic Medical Center,
University of Amsterdam,
Meibergdreef 15,
NL-1105 AZ Amsterdam, The Netherlands

J. Rydström
Biochemistry, Department of Chemistry,
University of Gothenburg,
Box 462,
S-405 30 Gothenburg, Sweden

Introduction

NADH:ubiquinone oxidoreductase (EC 1.6.5.3; Complex I) from bovine heart is the largest complex of the mitochondrial respiratory chain. Its mechanism of action has been, and still is, extensively studied. There is strong evidence that the bovine enzyme contains two FMN groups and has a specific site for NADPH (for overview see (Albracht 2010a, b)). At physiological pH the reaction between Complex I in bovine-heart submitochondrial particles (SMP) and excess NADPH (rate 40 s^{-1} at 22 °C) does not result in overall oxidation of NADPH by the respiratory chain. Likewise $K_3Fe(CN)_6$, the best artificial electron acceptor of the complex with NADH as electron donor, is not reduced when electrons are coming from NADPH. Hence, it has been proposed that Complex I contains two separate reactions sites for pyridine nucleotides each requiring a separate FMN group (Albracht and Hedderich 2000; Albracht 2010a, b). NADH reacts with the FMN group in the 51 kDa subunit (here referred to as FMN-b) resulting in oxidation of this substrate by the respiratory chain. NADPH reacts with the other FMN group (FMN-a) proposed to be bound to the conserved flavodoxin fold in the PSST subunit. Because this does not result in the overall oxidation of NADPH, the physiological relevance of this reaction has remained an enigma. Over the last 6 years certain developments in various, seemingly unrelated fields of research have inspired us to formulate a possible function.

Hypothesis in short

Our hypothesis is that the reaction of Complex I with NADPH can attenuate the levels of H_2O_2 generated by the enzyme during turnover with NADH under physiological conditions. When electrons come from NADH, FMN-a can be in the oxidized, semiquinone or reduced state, because electrons reach the flavin via Fe-S clusters, i.e. via $n=1$ redox groups (Fig. 1). With the NADPH/$NADP^+$ couple the flavin shuttles between FMN and $FMNH_2$ in an $n=2$ redox reaction. Under physiological conditions the semiquinone concentration will decrease when the NADPH/$NADP^+$ ratio increases. The membrane-bound Nnt has an apparent affinity for Complex I; it co-purifies with the complex in the classical purification procedure of Hatefi (Hatefi and Bearden 1976; Ragan and Widger 1975; Ragan 1976; Finel et al. 1992). Hence, it is proposed that the NADPH/$NADP^+$ ratio local to the site where NADPH reacts with Complex I, is dominated by the Δp-driven activity of Nnt. Reduced FMN-a cannot react with $K_3Fe(CN)_6$ and is not solvent accessible. Gaseous O_2 is considered to approach FMN-a through the hydrophobic tunnel in Complex I, which it has in common with [NiFe]-hydrogenases. Dioxygen can react fast with the flavosemiquinone radical to form superoxide ($O_2^{\bullet-}$). Its rate of reaction with $FMNH_2$ is very much slower (spin forbidden). The charged superoxide anion cannot leave the site through the hydrophobic gas tunnel. A caging effect will stimulate its spontaneous dismutation into H_2O_2 which then leaves the enzyme.

The hypothesis predicts that the association and co-operation between the two membrane-bound enzymes enables the protonmotive force (Δp), reflecting the energy status of the mitochondrion, to rapidly and specifically regulate the H_2O_2 generation by Complex I. Thus, at a high Δp Nnt will contribute to a high local NADPH/$NADP^+$ ratio, thereby attenuating the H_2O_2 production by Complex I, and *vice versa*. This specific H_2O_2 production, as well as the attenuation of it, is proposed to have a regulatory role in apoptosis and autophagy.

Dioxygen can also react with reduced FMN-b, as has been demonstrated with highly purified NADH dehydrogenase (Kussmaul and Hirst 2006). The redox state of FMN-b is controlled by the NADH/NAD^+ ratio and generated $O_2^{\bullet-}$ can rapidly diffuse from the solvent-accessible FMN-b into the bulk aqueous matrix medium.

Some general properties of the enzymes involved

Bovine-heart Complex I

Bovine Complex I (980 kDa) consists of 45 subunits (Fearnley and Walker 1992; Walker 1992; Hirst et al. 2003; Carroll et al. 2006). In its native form it contains two flavin molecules (FMN) and eight iron-sulphur (Fe-S) clusters, two of the [2Fe-2S] type and six of the [4Fe-4S] type (Fearnley and Walker 1992; Sazanov and Hinchliffe 2006; Albracht 2010a, b). It catalyzes the oxidation of NADH by Q_{10} (ubiquinone, also called coenzyme Q) and translocates ca. two protons per electron from the mitochondrial matrix (via the intermembrane space) to the cytosol (Wikström 1984; Galkin et al. 1999). The resulting Δp is used for the production in the matrix of ATP from ADP and phosphate. The ATP is subsequently transported to the cytosol by the adenine-nucleotide translocase (ANT) in exchange for cytosolic ADP, a process driven by the mitochondrial membrane potential ($\Delta\Psi_m$).

In the present paper the term ‘Complex I’ will be used for the enzyme in membrane preparations and for purified preparations that catalyze an inhibitor-sensitive (rotenone or piericidin A) NADH→ubiquinone activity without any reconstitution efforts. Purified preparations without this activity will be called ‘NADH dehydrogenase’, even although inhibitor-sensitive quinone reductase activity can often be induced by treatment with phospholipids. As discussed elsewhere (Albracht 2010a) nearly all NADH dehydrogenases contain only a single FMN.

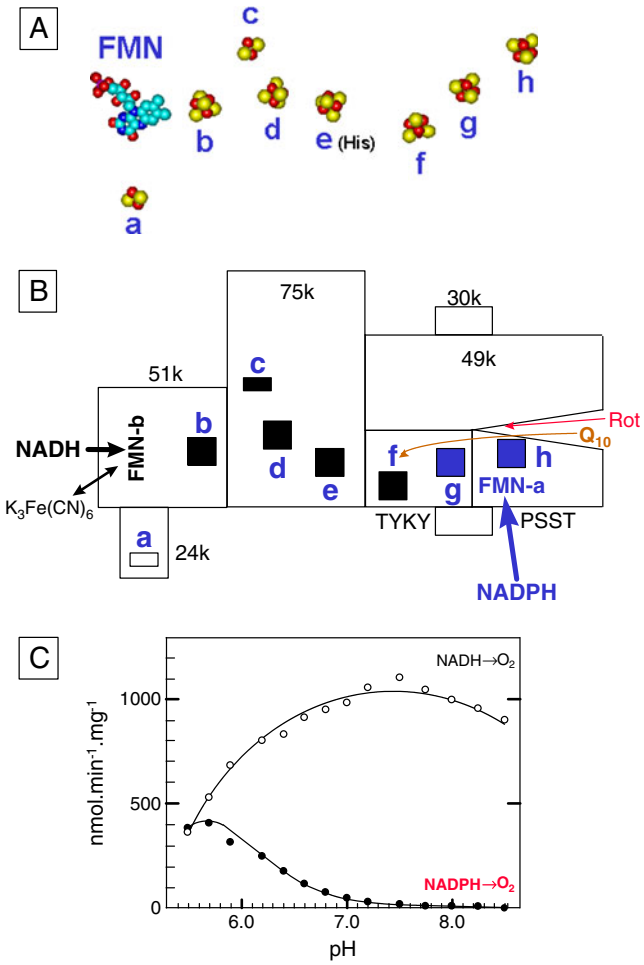

Fig. 1 The prosthetic groups in bovine Complex I, together with the proposed reaction sites of NADH, NADPH, rotenone and ubiquinone, and the observed pH dependencies of the NAD(P)H→O_2 reactions of submitochondrial particles. **A** Relative positions of the prosthetic groups in the hydrophilic domain of the *T. thermophilus* enzyme (coordinates taken from PDB entry 2fug (Sazanov and Hinchliffe 2006)). One [4Fe–4S] cluster in the largest subunit has been omitted because this cluster and the surrounding protein are not present in the 75 kDa subunit of bovine enzyme. The eight Fe-S clusters are termed here clusters *a* to *h*; the subunits harbouring them are indicated in (**B**). Clusters *a* and *c* are [2Fe–2S] clusters, the other ones are [4Fe–4S] clusters. All clusters but one are attached to the protein by four Cys residues; cluster *e* has one His and three Cys residues as ligands. Cluster *h* is special in that two of the four Cys residues are adjacent, a situation extremely rare in Fe-S proteins. **B** Modular representation of seven of the hydrophilic subunits of bovine Complex I and their prosthetic groups based on the information of the *T. thermophilus* enzyme. The second flavin in the native bovine enzyme, FMN-a, is supposed to be attached to the conserved flavodoxin fold in the PSST subunit (Albracht et al. 2003; Albracht 2010a, b). Note that the 30 kDa subunit, a polypeptide only found in proton-pumping hydrogenases and in Complex I and related enzymes, clamps the 49 kDa and TYKY subunits together. At neutral pH only the clusters *h* and *g* are rapidly reduced by NADPH (rate at least 40 s^{-1} at 22 °C) and electrons remain locked in the enzyme. The reaction is not affected by rotenone (Rot). Only one of the two binding sites of rotenone (site 1, on the surface of the 49 kDa subunit) is indicated here (for details see Fig. 2). At pH 6 and in the presence of rotenone, the clusters *e* and *f* are also reduced; under these conditions the reaction with NADPH has a rate of 100 s^{-1}. In the absence of rotenone, the reoxidation rate of the clusters *e* and *f* by Q_{10} is faster than their rate of reduction by NADPH at this pH. NADH reduces all clusters, except cluster *a* (rate at least 3,300 s^{-1} at 22 °C in the pH range of 5.5–8.3; rotenone insensitive). The reduction of FMN-a by NADH is inhibited by rotenone. The proposed reaction site of Q_{10} is also indicated; the quinone can approach this site via a hydrophobic tunnel (see Fig. 3 for further details). Reduction of both the clusters *f* and *g* is required for the reaction with ubiquinone (for details see (Albracht 2010a, b)). Squares stand for [4Fe–4S] clusters and rectangles for [2Fe–2S] clusters. **C** The pH dependencies of the NADH- and NADPH-oxidation activities catalyzed by bovine-heart SMP (at 30 °C) in which the transhydrogenase (Nnt) activity has been inactivated. Open circles, oxidation activities with 5 mM NADH; filled circles, oxidation activities with 5 mM NADPH (modified from (Albracht 2010b)). At neutral pH the NADPH→O_2 reaction is negligible with respect to the NADH→O_2 reaction

Recently the structures of the entire enzymes from *Thermus thermophilus* (bacterial enzyme, 4.5 Å resolution (Efremov et al. 2010)) and *Yarrowia lipolytica* (mitochondrial enzyme, 6.3 Å (Hunte et al. 2010)) have been resolved by X-ray diffraction. The global structures resemble the shape of the capital character L. The base of the L shape is anchored in the membrane and contains the hydrophobic subunits of the complex. The stalk of the L sticks out into the inner (cellular or mitochondrial) aqueous space and is composed of the hydrophilic subunits. A similar global surface shape has been determined with cryo electron microscopy (EM) for the mitochondrial enzymes from *Neurospora crassa* (Leonard et al. 1987; Hofhaus et al. 1991; Guénebaut et al. 1997), *Bos taurus* (Grigorieff 1998) and *Y. lipolytica* (Djafarzadeh et al. 2000), and for the bacterial enzymes from *Escherichia coli* (Guénebaut et al. 1998; Morgan and Sazanov 2008), *Aquifex aeolicus* (Peng et al. 2003) and *Paracoccus denitrificans* (Yip et al. 2011). As the enzymes contain different numbers of subunits, the surface-structural details may differ (Zickermann et al. 2009). The X-ray structure showed that the hand of most EM-derived surface structures was a mirror image of the correct structure (Efremov et al. 2010), as was independently reported by investigators using the cryo-EM technique (Dudkina et al. 2010). The structure of the membrane domain of the *E. coli* enzyme has also been resolved (3.9 Å) and is similar to that of the *T. thermophilus* enzyme (Efremov et al. 2010).

The structure of the hydrophilic domain of Complex I from *T. thermophilus* is known in more detail (3.3 Å resolution) (Sazanov and Hinchliffe 2006). This major achievement disclosed the long-awaited information on the relative positions of the subunits and prosthetic groups involved in electron transfer. In contrast to the native bovine enzyme, which contains 2 FMN groups (Albracht et al. 2003; Van der Linden et al. 2004), the crystallized *T.*

thermophilus enzyme has only one FMN and contains an extra [4Fe-4S] cluster in an extension of the largest subunit. The redox groups are approximately positioned along a straight line spanning a distance of ca. 90 Å. They form an 'electric wire' in the enzyme at an angle of ca. 120° (Efremov et al. 2010) to the plane of the membrane. The similarities between the global surface structures of Complex I from quite different organisms, as well as the high amino-acid sequence conservation between their prosthetic group-carrying subunits, has led to the consensus that the *T. thermophilus* structure may serve as a common template for the hydrophilic part of these enzymes. A schematic representation of the prosthetic groups in the bovine enzyme is shown in Fig. 1A and B.

Bovine-heart submitochondrial particles (SMP) can catalyze an NADPH→O_2 reaction; its rate is highly dependent on pH and peaks at pH 5.7 (Fig. 1C). At pH 5.5 the oxidation of NADPH is as fast as that of NADH; both reactions are at least 99% inhibited by rotenone or KCN. The K_m values for both substrates differ widely, being 7 to 8 μM for NADH (Hatefi and Hanstein 1973) and 550 to 570 μM for NADPH (Hatefi et al. 1962; Rydström et al. 1978).

In the *T. thermophilus* enzyme one side of the isoalloxazine ring of FMN (FMN-b) is solvent accessible. This is the site where NADH reacts. When bound, its nicotinamide ring is positioned on top of the isoalloxazine ring, like in many other pyridine-nucleotide-binding flavoenzymes (Berrisford and Sazanov 2009). This is also the proposed site of reaction of the artificial electron acceptor $K_3Fe(CN)_6$ (Fig. 1B). This explains the long known double-substrate inhibition kinetics of the NADH→ferricyanide reaction of the bovine enzyme (Dooijewaard and Slater 1976). At neutral pH the rate of this reaction is ca. 2,800 s^{-1} at 22 °C. Bovine Complex I does not show any NADPH→ferricyanide reaction (Hatefi et al. 1962; Ringler et al. 1960). This is in agreement with the proposal that NADPH does not react at FMN-b (Albracht 2010a, b).

Pre-steady-state kinetic experiments with SMP and excess NADPH, exclusively carried out in Amsterdam, showed that at pH 8 two of the Fe-S clusters in Complex I, the clusters *h* and *g* (Fig. 1B), are reduced by NADPH in a reaction with a rate of ca. 40 s^{-1} at 22 °C (Bakker and Albracht 1986; Van Belzen and Albracht 1989; Albracht 2010b). At this pH rotenone has no effect on the number of clusters reduced by NADPH or on their rate of reduction. The overall oxidation of NADPH by O_2 at pH 8 occurs with a rate of at most 1.4 s^{-1}, demonstrating that electrons from FMN-a and the clusters *h* and *g* do not readily reach the ubiquinone pool under these conditions. It should be recalled that the inhibitors piericidin A and rotenone have two binding sites in bovine Complex I (Fig. 2).

At pH 6.2, where the NADPH→O_2 reaction proceeds with a rate of at most 34 s^{-1} at 22 °C, the rate of the reaction between Complex I and NADPH is ca. 100 s^{-1}. At this pH, and in the presence of rotenone, this results in the complete reduction of the clusters *h*, *g*, *f* and *e* within 30 ms (Albracht 2010b). In the absence of the inhibitor only the clusters *h* and *g* remain reduced and the steady-state rate of oxidation is limited by the rate of reduction of cluster *f* by cluster *g* (Albracht 2010b). In the pH range of 5.5 to 8.3 NADH reduces FMN-b and all Fe-S, except cluster *a*,

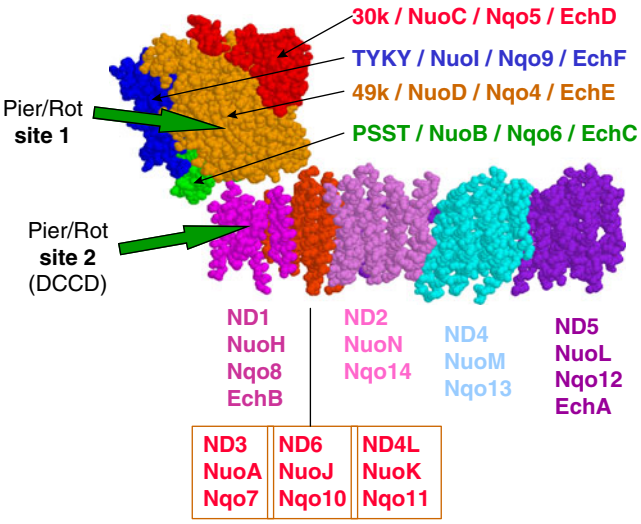

Fig. 2 Location of the inhibition sites of piericidin A, rotenone and *N*, *N*'-dicyclohexylcarbodiimide (DCCD) in mitochondrial Complex I. The image is based on the structure of the entire *T. thermophilus* enzyme (PDB entry 3m9s (Efremov et al. 2010)). All subunits of the membrane domain together with four subunits of the hydrophilic domain are shown. According to the 'steam-engine' model of Sazanov and co-workers (Efremov et al. 2010) conformational changes induced by electron transfer to ubiquinone catalyzed by these four hydrophilic subunits are relayed to the membrane domain. The latter domain performs the proton pumping. The nomenclature refers to homologous subunits from *B. taurus*, *E. coli*, *T. thermophilus* and, when applicable, to Ech (the proton-pumping [NiFe]-hydrogenase from *M. barkeri*), respectively. Both piericidin A (Pier) and rotenone (Rot) can bind stoichiometrically to two sites. The first site (site 1) is at the end of the hydrophobic tunnel close to the location in the 49 kDa subunit where in [NiFe]-hydrogenases the Ni-Fe site is bound (see Fig. 3 for further details). The second site (site 2) is at the ND1 subunit. Inhibition of the steady-state NADH oxidation at pH 8 in bovine SMP, pre-pulsed with NADH to activate Complex I, requires two molecules of piericidin A per Complex I (sites 1 and 2 occupied). SMP pre-pulsed with NADPH at pH 8.0 require only one inhibitor molecule for a complete inhibition of the initial NADH oxidation rate; binding at other sites is not observed. Within seconds, however, the rate increases to 50% of the maximal rate implying that now half or the SMP population has lost its inhibitor while the other half has both binding sites occupied (co-operative binding; for details see (Van Belzen et al. 1990; Albracht 2010b)). In the 'steam-engine' model of Sazanov and co-workers (Efremov et al. 2010) this might mean that structural changes in ND1 induced by reduction of Fe-S clusters not reducible by NADPH, and/or electron transfer to ubiquinone, is/are required for the simultaneous, tight binding of piericidin at both sites. Reduction with NADPH causes tight binding of only one inhibitor molecule (assumption: at site 1). DCCD binds to ND1 and blocks forward and reverse electrons transfer (Yagi 1987; Murai et al. 2007)

within 6 ms, even at 2 °C (Albracht 2010b); this is equivalent to a turnover number for NADH of at least 830 s^{-1}. Assuming a two- to three-fold change in rate for every 10 °C, the estimated turnover number at 22 °C would be at least 3,300 s^{-1}. The maximal rate of the NADH→O_2 reaction in Fig. 1C equals a turnover number of at most 153 s^{-1} at 22 °C. This demonstrates the well known property of Complex I in bovine-heart SMP that the rate of its reduction by NADH is much faster than its rate of reoxidation by ubiquinone. Thus, bovine Complex I comprises two separate FMN-containing dehydrogenase modules, one for NADH and the other for NADPH; both modules feed electrons to the TYKY subunit (Van Belzen and Albracht 1989; Albracht 2010a, b). Although rotenone and piericidin A have no effect on the rate or extent of reduction by NADH of FMN-b and the Fe-S clusters, the reduction of FMN-a is inhibited (for overview see (Albracht 2010a, b)).

The Δp-driven transhydrogenase (Nnt)

Nnt from bovine mitochondria is a homodimer with a monomer molecular mass of 109 kDa; it does not contain any prosthetic group. Each monomer consists of three domains: an N-terminal one (domain I, ca. 420 residues), which is hydrophilic and binds NAD(H); a central one (domain II, ca. 430 residues), which is hydrophobic and thought to contain 14 trans-membrane helices; and a C-terminal one (domain III, ca. 200 residues), which is hydrophilic and binds NADP(H) (Rydström 1972, 1977; Hatefi and Yamaguchi 1996; Bizouarn et al. 2000; Cotton et al. 2001; Jackson 2003; Pedersen et al. 2008). Its reaction can be written as:

$$NADH + NADP^+ + H^+_{out} \leftrightarrow NAD^+ + NADPH + H^+_{in}$$

Transhydrogenase can be driven by $\Delta\Psi_m$ as demonstrated in a reconstituted transhydrogenase-ATPase system (Eytan et al. 1990), but also by a pH gradient. The activity of a proton in the Nnt channel is affected by both $\Delta\Psi_m$ and ΔpH, i.e. for the same Δp a low $\Delta\Psi_m$ is compensated by a high ΔpH and *vice versa*, according to classical chemiosmotic coupling ($\Delta p\,(mV) = \Delta\psi_m - 59\Delta pH_{out-in}$). Ultimately, the conversion depends on the properties of the proton channel in Nnt and the functional groups there (e.g. His; cf the "well theory" meaning that in the center the only driving force will be a ΔpH (Bizouarn et al. 2000; Mitchell 2004)) and how these groups regulate the activity of the enzyme. In a reconstituted system Nnt is driven more efficiently by $\Delta\Psi_m$ than by a ΔpH. The magnitude of the Δp can drive the $((NADPH)/(NADP^+))/((NADH)/(NAD^+))$ ratio to values up to 500 (Rydström 1977; Hatefi and Yamaguchi 1996). In the absence of a Δp the reaction proceeds to an equilibrium point with K_{eq}=0.79, in agreement with the slight difference in redox potentials of the NADH/NAD^+ ($E^{0'}$=−320 mV) and NADPH/$NADP^+$ ($E^{0'}$=−325 mV) couples (Hatefi and Yamaguchi 1996).

The Nnt reaction is unique in the sense that it is the only known ion translocator in mitochondria in which the standard free energies of the products of the scalar chemical reactions are similar to those of the reactants (Pedersen et al. 2003).

Experimental and theoretical basis for the hypothesis

An experimental link between the action of Complex I and cancer

Bioenergetics of cancer cells; the Warburg phenotype

In 1924, Warburg and collaborators first reported that tumour tissue produced considerable amounts of lactic acid under aerobic conditions, in contrast to normal tissue that did so only in the absence of dioxygen (Warburg et al. 1924). They concluded that in tumours the oxidation rate of glucose ('Zuckeroxidation') cannot keep up with the rate of glycolysis ('Zuckerspaltung'). They found that especially in malignant tumours the ratio Zuckerspaltung/Zuckeroxidation was very high. Often this finding is referred to as 'the Warburg effect'. Strictly speaking it is not an 'effect' but a phenotype (the Warburg phenotype). Its use is also rather confusing because one of Warburg's other discoveries, the inhibitory effect of O_2 on photosynthesis (Warburg and Krippahl 1960), became known as 'the Warburg effect' in photosynthesis research (Ellyard and San Pietro 1969; Robinson et al. 1980).

Warburg hypothesized ('Hypothese über die Entstehung der Tumoren' (Warburg et al. 1924)) that tumours could be caused by chronic hypoxia of normal tissue. He assumed that some tissue cells survived because they had an enhanced capacity of (aerobic) glycolysis, whereas the majority of cells died due to shortage of O_2 because they did not have this property. This view (selective pressure) is still shared by present investigators (see e.g. (Borst and Rottenberg 2004; Mathupala et al. 2010)). A detailed insight into the precise causes for the metabolic reprogramming of cancer cells came from in depth genetic analyses of such cells (Parsons et al. 2008; Jones et al. 2008; Chin and Gray 2008; Stratton et al. 2009), but this will not be discussed here.

In vitro experiments. Effects of dichoro-acetate (DCA) on glucose metabolism in cancer cells

Michelakis and co-workers discovered that the abnormal glucose metabolism in cancer cells (Warburg phenotype)

can be normalized by a simple compound: dichloro-acetate (DCA) (Bonnet et al. 2007). It was demonstrated that the low level of glucose oxidation in cells of three human cancers (non-small-cell lung cancer, glioblastoma and breast cancer), having mitochondria with a hyperpolarized $\Delta\Psi_m$, is probably due to the constant inhibition of pyruvate dehydrogenase (PDH) by phosphorylation via one or more of its four kinases. Specific inhibition of the pyruvate dehydrogenase kinases (PDK) in these cancer cells by DCA, or by attenuation of the PDK2 activity by siRNA (Bonnet et al. 2007), caused (a/o): (i) A decrease of extracellular lactate; (ii) An increase of the intracellular pH; (iii) The decrease of the $\Delta\Psi_m$ in these cells to normal values (no effect in control cells); (iv) An increase of NADH in mitochondria isolated from the DCA-treated cancer cells; (v) A stimulation of electron transfer through the mitochondrial respiratory chain (also in control cells) with the concomitant increase (ca. 50%) in the cellular production of H_2O_2 (not in control cells). This increase was almost completely sensitive to rotenone whereas 2-thenoyl-trifluoroacetone (TTFA), an inhibitor of succinate: ubiquinone oxidoreductase (Complex II), had no effect; (vi) An increase in the outward K^+ current from the cells (no effect of DCA on control cells), leading to a hyperpolarization of the plasma membrane. This was largely inhibited by 4-aminopyridine, an inhibitor of voltage-dependent K^+ channels. The increased K^+ current was also blocked by rotenone or by micro-injected intracellular catalase, so it was apparently induced by an increased level of H_2O_2; (vii) An increase in the expression of the K^+ channel Kv1.5. In cancer cells this expression is lower than in normal ones; and (viii) A rotenone-sensitive decrease of the cytosolic Ca^{2+} level.

Thus, rotenone inhibited the DCA-induced increase in (cytoplasmic) H_2O_2, the DCA-induced increase in the outward K^+ current of the cancer cells and the DCA-induced decrease in the cytosolic Ca^{2+} concentration (Bonnet et al. 2007). The primary DCA effects on these cells were rather rapid, i.e. the normalization of the $\Delta\Psi_m$, as well as the induction of the K^+ current and the decrease of cytoplasmic Ca^{2+}, occurred within 5 min (and persisted after 48 h). We also note that the DCA-induced normalization of the hyperpolarized $\Delta\Psi_m$ was accompanied by a increase of the intracellular pH. This strongly suggests that the cancer-cell mitochondria had an abnormally high Δp.

The (hyperpolarized) $\Delta\Psi_m$ in the cancer cell lines was hardly affected by KCN, but this inhibitor greatly decreased the (normal) $\Delta\Psi_m$ of DCA-treated cells. Hence, the authors concluded that the $\Delta\Psi_m$ hyperpolarization of non-treated cancer cells was apparently not caused by electron transfer. Uncoupler diminished the $\Delta\Psi_m$ of cancer cells, of DCA-treated cancer cells and of normal cells to the same low level (Bonnet et al. 2007). Moreover, it was shown that DCA induced apoptosis and decreased proliferation of the cancer cells, i.e. it induced an overall cell death. The experiments suggested that the DCA-induced apoptosis was achieved via two pathways, the mitochondria-dependent one (ca. 65%) and the plasmalemmal one (ca 35%). Noteworthy is that the DCA-induced changes in both processes were inhibited by rotenone. This specific effect of DCA has now been confirmed in several other studies, e.g. with two more human cancers, endometrical adenocarcinoma (uterin corpus) and prostate cancer (Wong et al. 2008; Cao et al. 2008; Michelakis et al. 2008), in rat metastatic breast cancer cells (Sun et al. 2010) and in colorectal cancer cells (Madhok et al. 2010) (for overview see e.g. (Papandreou et al. 2010)). Presently, DCA is being used in clinical trials (http://clinicaltrials.gov).

The crystal structure of PDK1 shows that DCA can bind to its N-terminal domain. The binding induces conformational changes relayed to the nucleotide and lipoyl-binding pockets of the protein (Kato et al. 2007), whereby a correct structure of a particular motif (DW-motif) in the C-terminus is essential (Li et al. 2009). Once the PDK is inhibited in the cell, the phosphorylated, inactive PDH can be rapidly activated again by the action of a specific phosphatase (Whitehouse et al. 1974). Especially PDK3, upregulated in cancer cells and the only enzyme of the four PDKs that is not inhibited by pyruvate, may play a dominant role in the suppression of the PDH activity (Lu et al. 2008).

Because many of the effects of DCA on cancer cells were largely inhibited by rotenone, Bonnet et al. proposed a 'complex I-centered' mechanism to explain them (Bonnet et al. 2007; Michelakis et al. 2010). Enhanced mitochondrial NADH levels would lead to enhanced production of reactive oxygen species (ROS) by Complex I and this would damage its Fe-S clusters, in fact a suicidal action. In turn, this would lead to a diminished $\Delta\Psi_m$. As discussed later on, we consider this explanation less likely.

In vivo experiments with DCA

In rat-model experiments DCA caused an immediate halt in tumour growth and a significant decrease in tumour size after 1 week of treatment, without apparent toxic effects on normal tissue (Bonnet et al. 2007). A recent study of the effects of DCA in patients with brain tumours (Michelakis et al. 2010) corroborated and extended the earlier in vitro and rat-model ones (Bonnet et al. 2007). The results were consistent with an inhibition of angiogenesis, induction of apoptosis and suppression of proliferation in the tumours by the DCA treatment. In accordance with earlier reports (reviewed by (Pastorino and Hoek 2008; Mathupala et al. 2009)) hexokinase-II was found to be bound to mitochondria in tumour tissue (but not in normal tissue). Hexokinase-II is upregulated in cancer cells and binds to

the outer-membrane voltage-dependent anion channel (VDAC), of which the ATP-ADP translocase (ANT) is a part. It has been proposed that this hexokinase taps off ATP right at the spot where it comes out of the mitochondrion (Pastorino and Hoek 2008; Mathupala et al. 2009). DCA removed this binding (Michelakis et al. 2010). In addition it was found that DCA induced activation of the pro-apoptotic tumour-suppressor transcription factor p53 and increased the level of downstream p21, an activator of many protein kinases (Van den Broeke et al. 2010). Recent evidence has shown that, in addition, p53 binds to, and inhibits the activity of, glucose 6-phosphate dehydrogenase so that the pentose phosphate pathway, the major producer of cytosolic NADPH, becomes compromised (Jiang et al. 2011). The study of Michelakis (Michelakis et al. 2010) demonstrated that the amounts of DCA required to inhibit PDK in cancer patients cause no or only very mild reversible neurotoxic side effects.

DCA also decreased the level of HIF-1 (hypoxia-inducible transcription factor) in the nucleus (Michelakis et al. 2010). HIF-1 is a most important transcription factor that safeguards cellular ATP production in healthy individuals under hypoxic conditions. It is a heterodimeric protein and its concentration in the cell is regulated via the level of one of the subunits, HIF-1α. Under normoxic conditions two specific proline residues in the HIF-1α subunit are readily hydroxylated by a specific enzyme (HIF-hydroxylase) containing a prolyl 4-hydroxylating domain as discovered in 2001 (Ivan et al. 2001; Jaakkola et al. 2001). Like the related pro-collagen prolyl 4-hydroxylase, this enzyme requires 2-oxoglutarate and O_2 as substrates and ascorbate (vitamin C) as an activator (Knowles et al. 2003; Vissers et al. 2007; Kaelin and Ratcliffe 2008) also in vivo (Kuiper et al. 2010). For the pro-collagen enzyme from chick embryos (reaction: 2-oxoglutarate+O_2+Pro-R→succinate+CO_2+4-OH-Pro-R) it has been demonstrated by EPR measurements that ascorbate is required to keep the iron ion in the active site in the ferrous (Fe^{2+}) state (De Jong et al. 1982; De Jong and Kemp 1984). Ferrous iron can bind and activate O_2, whereas ferric iron (Fe^{3+}) cannot. In the absence of the target 'Pro' substrate a direct oxidation of ascorbate takes place (reaction: 2-oxoglutarate+Asc+O_2→succinate+CO_2+dehydroAsc) and catalysis (of this specific reaction) continues (De Jong and Kemp 1984). If ascorbate is absent as well, then catalysis stops due to oxidation of Fe^{2+}.

Hydroxylation of either of the Pro residues in HIF-1α generates a binding site for the 'von Hippel-Lindau' tumour suppressor protein (pVHL), a component of the ubiquitin ligase complex. This results in poly-ubiquitination of HIF-1α, which is then subject to degradation by the 26S proteasome (Kaelin and Ratcliffe 2008). Under normoxic conditions (and in the presence of ascorbate) the active heterodimeric HIF-1 protein is hardly formed. In normal tissue the O_2 concentration (10–30 μM) is well below the K_m of the active HIF-hydroxylase for O_2 (90–100 μM) (Kaelin and Ratcliffe 2008). Hence, the reaction rate is nearly directly proportional to the O_2 concentration and so it slows down under hypoxic conditions. A decreased 2-oxoglutarate level will amplify this effect. Interestingly, a deficiency of ascorbate in neutrophils from vitamin-C-deficient mice leads to HIF-1α formation even under normoxic conditions. For these white blood cells ascorbate is essential for their spontaneous apoptosis (Vissers and Wilkie 2007). The active HIF-1 heterodimer regulates the expression of well over hundred nuclear genes, e.g. it causes the upregulation of genes encoding PDK1, PDK3 (Kato et al. 2007; Lu et al. 2008), and proteins and enzymes involved in glucose uptake, glycolysis, erythropoiesis, angiogenesis, and autophagy of mitochondria (Semenza 2008b). This is accompanied by downregulation of mitochondrial biogenesis (Kaelin and Ratcliffe 2008; Mole et al. 2009). As a result, the bioenergetic phenotype of the cell shifts from a glucose-oxidative type (bulk of ATP produced by mitochondria) to a glycolysis type (increased ATP production in the cytosol), in agreement with Warburg's observations (Warburg 1927, 1954).

It is worthwhile to mention that in addition to the bioenergetic phenotype (Warburg phenotype), that may be normalized by DCA (Bonnet et al. 2007; Michelakis et al. 2010), many tumours also show an immunological phenotype, i.e. they manage to cripple the immune system. A simple re-activation appears to be an extremely efficient novel method to eradicate many cancers (see e.g. (Yamamoto et al. 2008, 2009) and reference therein).

Hyperpolarization of the mitochondrial inner membrane observed in cancer cells

Mitochondria in most types of cancers share an interesting bioenergetic property: they have a much higher $\Delta\Psi_m$, of at least 60 mV, than mitochondria in normal cells. Because the outside of the inner membrane is positive, while the matrix side is negative, this has been measured by the accumulation of positive fluorescent dyes like Rhodamine 123 (Chen 1988). Although not discussed in (Chen 1988), where 200 different cancer cell lines were investigated, it is less likely that this increased $\Delta\Psi_m$ is caused by respiration, because the rate of pyruvate oxidation in mitochondria in cancer cells is lower than that in normal cells (Warburg et al. 1924; Warburg 1927; Bonnet et al. 2007). Also the observation that KCN and TTFA had no effect on the $\Delta\Psi_m$ in cancer cells (Bonnet et al. 2007) is in agreement with the idea that the increased $\Delta\Psi_m$ is not caused by respiration. It should be mentioned, however, that only a low dose (5 μM) KCN was used in these experiments. Cyanide inhibition of cytochrome *c* oxidase is easily reversed by pyruvate

(Cittadini et al. 1971) because pyruvate reacts non-enzymically with cyanide to form cyanhydrin (Warburg 1948). Even although cyanide did decrease the $\Delta\Psi_m$ in DCA-treated cells, it could well be that the steady-state pyruvate concentrations in DCA-treated cells was lower than that in non-treated cells. Also the used concentration of TTFA (1 μM) was two orders of magnitude lower than that usually applied to inhibit succinate dehydrogenase (Ackrell et al. 1977). In contrast, and as discussed above, rotenone is a strong and specific inhibitor of Complex I and is effective in very low concentrations (Ernster et al. 1963; Gutman et al. 1970). Nevertheless, we support the view (Bonnet et al. 2007; Michelakis et al. 2010) that the hyperpolarization of $\Delta\Psi_m$ in cancer cells, representing an abnormally high Δp as discussed above, is presumably not ruled by the mitochondrial respiration. Instead we will argue that conditions in the cytosol are responsible for that.

Pedersen (Pedersen 1978) has argued that hexokinase, which in cancer cells is also bound to the outside of the mitochondria, may channel large amounts of glucose-6-phosphate into the upregulated glycolysis. The fast trapping of P_i in glucose-6-phosphate might then limit mitochondrial ATP synthesis and, in turn, this might lead to an increased $\Delta\Psi_m$.

Another possibility, one that we favour, is that the cytosolic ATP/ADP ratio driven by the upregulated glycolysis in malignant tumour cells is considerably higher than that in normal cells. The release of inhibition of PDH by DCA in cancer cells increased the glucose-oxidation rate by ca. 23% (Bonnet et al. 2007) to 44% (Michelakis et al. 2010). This caused a decrease, not an increase, of the $\Delta\Psi_m$ and an increase of the intracellular pH in agreement with the assumption that the abnormally high Δp was not caused by respiration. We note that the quickness of the DCA effect on the $\Delta\Psi_m$ (apparent within 5 min) nicely agrees with the onset of the activation of PDH by DCA in perfused rat heart (caused by DCA-induced inhibition of PDK) which was apparent after ca. 3 min (Whitehouse et al. 1974). Therefore we are inclined to think that the normalization of the $\Delta\Psi_m$ (from hyper- to normal polarization) by DCA in the experiments from Bonnet et al. (Bonnet et al. 2007) coincided with the stimulation and normalization of the PDH activity. DCA also increases respiration in normal cells (Whitehouse et al. 1974). However, this is not accompanied by a change in $\Delta\Psi_m$ (Bonnet et al. 2007).

We also note that the effects of DCA on cancer-cell metabolism are similar to those induced by knocking out lactate dehydrogenase in mammary tumour cells. In that case pyruvate is forced to be oxidised by the mitochondria which resulted in increased respiration, a fall in $\Delta\Psi_m$ and a diminished tumourigenicity. Under hypoxic conditions (0.5% O_2), the growth rate of such cells was diminished by two orders of magnitude (Fantin et al. 2006). Similar effects could be induced by a specific inhibitor of lactate dehydrogenase (FX11, 3-dihydroxy-6-methyl-7-(phenylmethyl)-4-propylnaphthalene-1-carboxylic acid). This inhibitor also reduced the ATP levels in the cancer cells. In addition it inhibited the progression of human lymphoma and pancreatic cancer xenografts (Le et al. 2010).

An increase of the pyruvate-oxidation rate in cancer cells induced by DCA will cause a sharp decrease in the cytosolic lactate production. In turn, this leads to a sudden (large) increase in the cytosolic NADH/NAD^+ ratio. Normalization of this ratio then depends on the mitochondrial H-shuttles (glycerol-3-phosphate and malate-aspartate shuttles). Although the shuttles have not been considered as a rate-limiting factor in the control of glucose oxidation in tumour cells (Pedersen 1978) it must be stressed that flux through the shuttles is not only dependent on the shuttle enzyme activities but also on the steady state concentrations of the shuttle intermediates under these conditions. In the presence of DCA, a decreased capacity of these shuttles in tumour cells, a/o caused by a lower mitochondrial mass and respiration (which can be dramatic (Zhang et al. 2008)), will lead to a shortage of cytosolic NAD^+ and a diminished activity of the genetically upregulated aerobic glycolysis system. In turn, this will result in a decrease of the cytosolic ATP/ADP ratio under these conditions. A hyperpolarized $\Delta\Psi_m$ caused by a glycolysis-powered elevation of the cytosolic ATP/ADP ratio is also in agreement with the observation that the aggressiveness and the metastatic potential of colonic carcinoma cells with a high $\Delta\Psi_m$ are greater than those of carcinoma cells with a lower $\Delta\Psi_m$ (Heerdt et al. 2006).

An abnormally high Δp, readily measured as a hyperpolarized $\Delta\Psi_m$, will diminish the activities of the proton-translocating Complexes I, III and IV of the respiratory chain. At the same time, it will stimulate the activity of Nnt, especially at higher NADPH concentration. Our hypothesis (discussed in detail later on) predicts that this would result in an (hyper)increase of the NADPH/$NADP^+$ ratio near the NADPH site of Complex I. Thus, the excessive $\Delta\Psi_m$ of most cancers may lead to a severe attenuation of the H_2O_2 production by Complex I, i. e. the sheer power of the aerobic glycolysis in the cancer cells forces the mitochondria to limit their Complex-I-produced H_2O_2 and this may enable the cells to, a/o, evade apoptosis. The hypothesis also predicts that the DCA-induced decrease of the $\Delta\Psi_m$ in cancer cells is the trigger for the increase in the H_2O_2 generation by Complex I.

It is conceivable that a high cytosolic ATP/ADP ratio in cancer cells may also lead to an increased ATP/ADP ratio in the mitochondrial matrix. An elevated ATP level in the matrix facilitates the phosphorylation of PDH by PDK, as convincingly shown by (Taylor et al. 1975), and so it will

add to the genetically increased suppression of the pyruvate-oxidation rate.

Reactions of dioxygen with bovine Complex I

On the reactions of O_2 with biomolecules

Dioxygen has an electronic ground state with two unpaired electrons in two antibonding π^* orbitals and hence it is paramagnetic (S=1). The reactions of this triplet molecule with most organic molecules, which have a singlet (S=0) ground state, are kinetically very slow because they are spin forbidden. In addition, the one-electron reduction potential of O_2 ($O_2+e^- \rightarrow O_2^{\bullet-}$) is unfavourably low, further restricting possible reactivity. Although biochemicals like ascorbate, dithiothreitol, cysteine and reduced flavin are said to be auto-oxidizable, the reactions are spin restricted and a catalyst, usually traces of a transition metal ion like Fe, Cu or Mn, are required for the reaction to proceed (Miller et al. 1990). In biochemical experiments extraneous iron (often called 'dirty iron', i.e. all iron except that inherent to proteins) is nearly always present and is complexed to buffers and virtually all proteins (causing the well known g=4.3 EPR signal). When working with tissue, mitochondria or SMP there is no lack of (complexed) iron ions and this is why auto-oxidation of thermodynamically-suited molecules may occur. Triplet dioxygen can readily react with radical forms (S=1/2) of biomolecules with a sufficiently low redox potential to form $O_2^{\bullet-}$. Because superoxide is a doublet (S=1/2) species, this reaction is spin-allowed. Under physiological conditions the rate is often only limited by diffusion (Miller et al. 1990). Under special conditions, e.g. photosensitized reactions with triplet O_2, singlet dioxygen can be formed. This S=0 molecule readily react with many biomolecules. Thermal excitation of O_2 to singlet dioxygen, or of combustible material to the triplet state, also results in a fast reaction of mixtures of the two (fire).

Usually, the incompletely reduced oxygen species $O_2^{\bullet-}$, H_2O_2 (hydrogen peroxide) and $HO^{\bullet}$ (hydroxyl radical), are collectively called 'reactive oxygen species' (ROS). Because of its rapid reaction with radical forms of suitable biomolecules, dioxygen itself is also a reactive oxygen species. The so-called ROS production in biological systems mainly concerns superoxide ($O_2^{\bullet-}$) and/or hydrogen peroxide (H_2O_2) but, of course, not dioxygen. From the four oxygen species, only the $HO^{\bullet}$ radical can attack virtually all chemical bonds in biomolecules. The hydroxyl radical can only be produced from O_2 by three sequential one-electron reduction steps. The reduction of O_2(g) to $O_2^{\bullet-}$ has a low oxidation-reduction potential at pH 7 ($E^{0'}$=−0.33 V). In aqueous solution this potential is ca. −0.17 V (Miller et al. 1990; Koppenol et al. 2010). For singlet O_2, both potentials are 1 V higher (Koppenol et al. 2010). The reduction of $O_2^{\bullet-}$ to H_2O_2 proceeds with an $E^{0'}$ of ca. +0.93 V, whereas the reaction $H_2O_2+1e^-+H^+ \rightarrow H_2O+HO^{\bullet}$ has an $E^{0'}$ of ca. +0.36 V. The latter reaction easily proceeds in the presence of Fe^{2+} ions (Fenton chemistry). The one-electron reduction of $HO^{\bullet}$ to water occurs with an $E^{0'}$ of +2.31 V, making it by far the strongest oxidant of all oxygen species (for a complete list of the redox potentials, see e.g. (Koppenol et al. 2010)).

The one-electron reduction of $O_2^{\bullet-}$ (S=1/2) gives H_2O_2 (S=0); hence the superoxide anion can only react fast with electron-donating molecules in the doublet state. The reaction between two $O_2^{\bullet-}$ anions is not occurring due to Coulomb repulsion. In fact, the rate of the spontaneous superoxide dismutation reaction is pH dependent (McCord and Fridovich 1978). Because the $HO_2^{\bullet}$ radical has a pK_a of 4.8, the major dismutation reaction at physiological pH is

$$HO_2^{\bullet} + O_2^{\bullet-} + H^+ \rightarrow H_2O_2 + O_2$$

Although the rate constant for this reaction is large (ca. 10^7 $M^{-1}.s^{-1}$) (McCord and Fridovich 1978), the low concentration of $O_2^{\bullet-}$ and in particular that of $HO_2^{\bullet}$ under physiological conditions make that this spontaneous dismutase reaction would be insignificant in the absence of any catalysts, i.e. the half-life time of $O_2^{\bullet-}$ could be considerable (up to minutes or hours). Superoxide dismutases react solely with $O_2^{\bullet-}$ in two successive steps; sum reaction:

$$O_2^{\bullet-} + O_2^{\bullet-} + 2H^+ \rightarrow H_2O_2 + O_2$$

The rate constant of this reaction (ca. 2×10^9 $M^{-1}.s^{-1}$) approaches the value set by diffusion. When present, nitric oxide ($NO^{\bullet}$, a radical formed from arginine by nitric oxide synthase), reacts with $O_2^{\bullet-}$ in a diffusion-controlled reaction to form the highly reactive, toxic peroxinitrite ($ONOO^-$).

Most relevant for possible damage by ROS to the mitochondrial energy metabolism is the very fast reaction of $O_2^{\bullet-}$ with the $[4Fe–4S]^{2+}$ cluster in active aconitase in the matrix. Superoxide oxidizes the cluster to the $[4Fe–4S]^{3+}$ state which is not stable and decomposes into a $[3Fe–4S]^{+}$ cluster and Fe^{2+}, resulting in an inactive enzyme. The second-order rate constant for this reaction is 10^6 to 10^7 $M^{-1}.s^{-1}$ (Flint et al. 1993). The formed H_2O_2 reacts with Fe^{2+} to produce $HO^{\bullet}$ (Vásquez-Vivar et al. 2000), but this does not cause any irreversible damage in the enzyme (Flint et al. 1993; Vásquez-Vivar et al. 2000). Both H_2O_2 and O_2 can also oxidize the $[4Fe–4S]^{+}$ cluster, but the rates are much smaller (10^3 $M^{-1}.s^{-1}$ and ca. 10^2 $M^{-1}.s^{-1}$, respectively (Flint et al. 1993)). Other [4Fe–4S] cluster-containing hydrolyases are inactivated similarly (Flint et al. 1993), e.g. the cytosolic aconitase, which in fact is an iron-regulatory protein (also called iron-response element binding protein, IRE-BP). The cluster-containing protein has aconitase activity and cannot bind to IREs, stem-loops in mRNA for

a variety of Fe-S proteins. Oxidation of the cluster leads to a complete loss of it. The apo-enzyme has no aconitase activty, but can bind to IREs (Beinert et al. 1996). Thus, O_2, H_2O_2 and in particular $O_2^{\bullet-}$ in the cytosol can have a prominent effect on the iron metabolism of the cell.

A hydrophobic gas tunnel common to both [NiFe]-hydrogenases and Complex I

It is now quite clear that the structure of the PSST subunit of Complex I is highly similar to that comprising the flavodoxin domain in the small subunit of standard [NiFe]-hydrogenases (Fig. 3). In addition, the structure of the 49 kDa subunit is similar to that of the large subunit of such hydrogenases (Sazanov and Hinchliffe 2006; Fontecilla-Camps et al. 2007). Also the relative positions of these subunits are the same. This was already predicted from extensive sequence comparisons (Albracht and Hedderich 2000). The interface surface between the two subunits in standard hydrogenases is very large (Volbeda et al. 1996) (see Fig. 3B). The PSST subunit misses the C-terminal domain, including two Fe-S clusters, of the related small subunit in standard hydrogenases (Fig. 3C). This is also the case for the small subunits of two particular [NiFe]-hydrogenases, namely for HoxY from the soluble NAD^+-reducing enzyme from *Ralstonia eutropha* and for EchC in the proton-pumping hydrogenase Ech (*E. coli* hydrogenase-3-type hydrogenase) from *Methanosarcina barkeri*. As a result, part of the surface on the 49 kDa subunit in Complex I (Fig. 3C), and of the large hydrogenase subunits HoxH of the *R. eutropha* enzyme and EchC in the *M. barkeri* enzyme, would be exposed to the bulk medium. As predicted (Albracht and Hedderich 2000), the TYKY subunit occupies this surface area on the 49 kDa subunit in Complex I and at the same time 're-installs' the two Fe-S clusters (Fig. 3C). In the *R. eutropha* soluble hydrogenase this surface area is predicted to be covered by the HoxU subunit and in the Ech by the EchF subunit (Albracht and Hedderich 2000; Albracht 2010a, b).

The structural comparison of Complex I and [NiFe]-hydrogenases (Sazanov and Hinchliffe 2006; Fontecilla-Camps et al. 2007) also disclosed that a hydrophobic gas tunnel formed by the small and the large subunits in [NiFe]-hydrogenases, a tunnel that leads to the Ni-Fe site, overlaps with a much wider hydrophobic tunnel in Complex I, now known to begin at the membrane surface (Efremov et al. 2010; Hunte et al. 2010). In Complex I it is a possible binding site for (part of) the long hydrophobic tail of Q_{10} (Sazanov and Hinchliffe 2006). It may also allow the hydrophobic inhibitors rotenone and piericidin A to reach one of their specific binding sites close to the centre of the 49 kDa subunit (site 1,

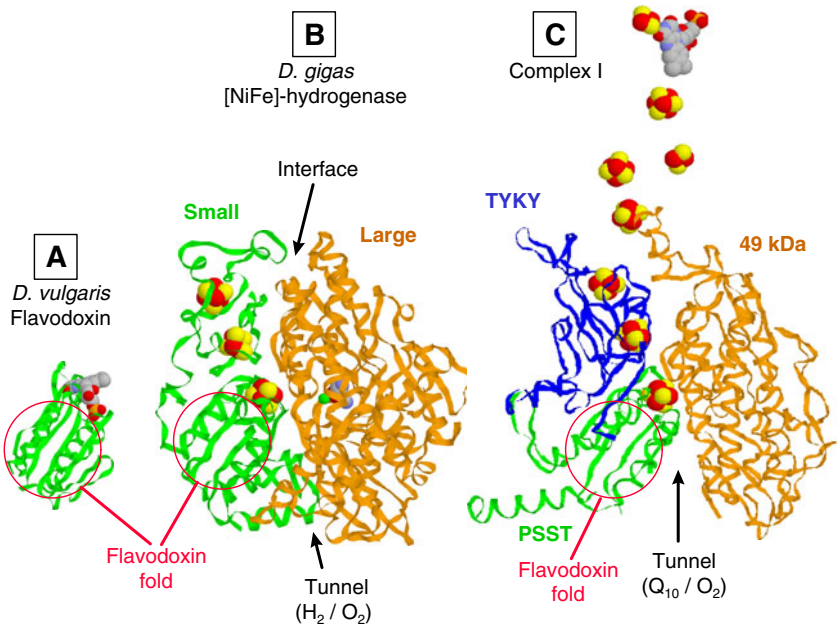

Fig. 3 Comparison of the structures of flavodoxin from *Desulfovibrio vulgaris* Hildenborough (**A**), *D. gigas* [NiFe]-hydrogenase (**B**) and part of the hydrophilic domain of Complex I from *T. thermophilus* (**C**). For Complex I only the structures of the TYKY (Nqo9), PSST (Nqo6) and 49 kDa (Nqo4) subunits are shown as ribbons. Prosthetic groups are depicted in Van Der Waals radii. Flavodoxin contains one FMN group. Hydrogenase contains two [4Fe–4S] clusters, with a [3Fe–4S] cluster in between, in the small subunit, and the Ni–Fe(CO)$(CN)_2$ active site (Happe et al. 1997) in the large subunit. The prosthetic groups in Complex I are as in Fig. 1A. In (**B**) and (**C**) the images are positioned such that the Fe-S clusters in the TYKY and PSST subunits of Complex I are aligned with the three Fe-S clusters in hydrogenase. Co-ordinates were taken from the structure files (PDB entries: 3fx2 for flavodoxin (Watt et al. 1991), 2frv for hydrogenase (Volbeda et al. 1996) and 2fug for Complex I (Sazanov and Hinchliffe 2006)). The red circles indicate the position of the flavodoxin fold. The positions of the large interface between the hydrogenase subunits and of the hydrophobic tunnels in (**B**) and (**C**) are also indicated

see Figs. 1 and 2). In the *Desulfovibrio gigas* hydrogenase (Volbeda et al. 2005) H_2 gas diffuses through the gas tunnel up to the Ni-Fe active site. Also O_2(g) is able to do this and can then be reduced to hydroxide or peroxide at the Ni-Fe site (George et al. 2004; Kurkin et al. 2004; Armstrong and Albracht 2005; Vincent et al. 2005; Van der Linden et al. 2006). In [NiFe]-hydrogenases this reaction is not merely a 'leak reaction'; instead it enables these enzymes to quickly switch off their activity by occupying the H_2-reaction site at nickel with a hydroxide or peroxide group. In that way these enzymes avoid the highly-exothermic Knallgas reaction to take place at the Ni-Fe site and prevent wasting of precious H_2 for the bacterial host. For Complex I we propose that the diffusion of O_2(g) into the hydrophobic tunnel enables its reaction with the semiquinone and reduced forms of FMN-a (Figs. 3 and 4). We consider this to be a constitutive functional reaction of the enzyme and not simply an electron-leakage reaction.

It is conceivable that the wide hydrophobic tunnel formed by the PSST and 49 kDa subunits may also bind one or more phospholipids molecules. Removal of phospholipids from this tunnel may explain the loss of reaction with ubiquinone and the loss of the specific binding of the inhibitors rotenone and piericidin A. Apparently the correct structure of the electronic heart of Complex I, i.e. the module formed by the TYKY, PSST, 49 kDa and 30 kDa subunits (Albracht 2010a) (Fig. 2) stabilized by phospholipids and Q_{10}, is critically dependent on the presence and correct structure of each of its components. This delicate structural interdependence may also explain why the removal of phospholipids may result in loss of FMN-a (Albracht et al. 2003; Albracht 2010a) and affects the properties (e.g. the EPR linewidth and apparent midpoint potential) of the clusters *f* and *g* (1.92 line) in bovine

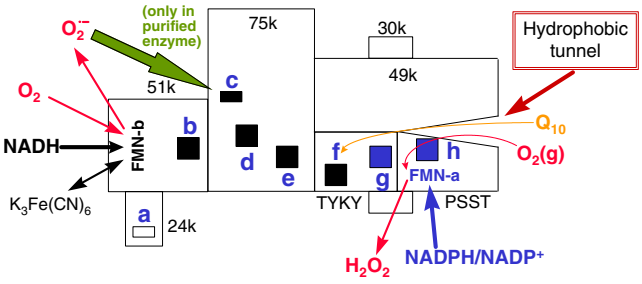

Fig. 4 Proposed reactions of dioxygen with Complex I. FMN-b is solvent accessible and dissolved oxygen reacts here with $FMNH_2$ (spin forbidden). The produced $O_2^{\bullet-}$ rapidly diffuses into the bulk aqueous matrix phase. In purified preparations it attacks and modifies the [2Fe–2S] centre in cluster *c*. FMN-a is not solvent accessible. Gaseous dioxygen approaches through the hydrophobic tunnel and reacts with $FMNH^{\bullet}$ (spin allowed) or $FMNH_2$. The formed $O_2^{\bullet-}$ cannot escape via the hydrophobic tunnel and experiences a caging effect. Spontaneous dismutation as well as subsequent reduction by reformed $FMNH^{\bullet}$ (both spin allowed) result in H_2O_2 formation which escapes from the enzyme. See text for further details

Complex I (Ragan and Racker 1973; Ohnishi et al. 1974; Finel et al. 1992, 1994) and the *E. coli* enzyme (Sinegina et al. 2005). It may further explain e.g. why some point mutations in the 49 kDa subunit of the *Y. lipolytica* Complex I resulted in the disappearance of EPR signals from Fe-S clusters in other subunits (Kashani-Poor et al. 2001; Grgic et al. 2004; Zwicker et al. 2006; Tocilescu et al. 2010), whereas other mutations had no effect (Tocilescu et al. 2007). Similar observations have been made with the *E. coli* enzyme (Belevich et al. 2007).

Reactions of O_2 with purified Complex I and NADH dehydrogenases

The properties of the classical intact Complex I from bovine heart were first described by Hatefi and co-workers in 1962 (Hatefi et al. 1962). Purification involved the use of the natural bile detergents deoxycholate and cholate in combination with inorganic salts. Hatefi's Complex I contained ca. 22% lipids (w/w) and 2.8–3.2 molecules of Q_{10} per FMN (Hatefi et al. 1962), i.e. 5.6–6.4 molecules Q_{10} per Complex I. It catalyzed the rotenone-sensitive reduction of ubiquinone by NADH. Another classical preparation, containing much less phospholipids, was obtained from SMP by the action of the phospholipase A (from *Naja naja* venom) (Ringler et al. 1960, 1963; Cremona and Kearney 1964; Lusty et al. 1965). Its redox-linked properties, i.e. FMN, Fe and acid-labile sulphur content, reduction of $K_3Fe(CN)_6$ by NADH, and the EPR properties were highly similar to those of Hatefi's Complex I. However, it did not contain Q_{10}, nor did it react with quinones in a rotenone- or piericidin-A-sensitive way. This preparation was usually called the high-molecular weight type NADH dehydrogenase, but we will refer to it as Singer's NADH dehydrogenase. These classical preparations contained two FMN groups per enzyme molecule (Albracht et al. 2003).

When Hatefi's Complex I (16–18 Fe atoms per FMN; see below) was further purified, using dodecyl maltoside, glycerol, a sucrose gradient and column chromatography, a fairly active preparation (NADH→Q_1 activity 0.516 μmol.min^{-1}.mg^{-1}, i.e. 9 s^{-1} at 20 °C, pH 8, 85% rotenone sensitive) was obtained with 28 Fe atoms (and 3 Q_{10} molecules) per FMN (Nakashima et al. 2002), indicating the loss of FMN-a. More recently the same laboratory, using a different preparation procedure, purified a more active enzyme (NADH→Q_1 activity 1.27 μmol.min^{-1}.mg, i.e. 21 s^{-1} at 20 °C, pH 8, 90% rotenone sensitive; the mentioned activity, 1.27 μmol.min^{-1}.μmol^{-1}, must have been a printing error) with 30 Fe atoms (and 1 Q_{10} molecule) per FMN (Shinzawa-Itoh et al. 2010). This preparation will be referred to as Yoshikawa's Complex I.

A monodisperse preparation of the bovine enzyme has been obtained by the group of Hirst using synthetic

detergents, salts and column chromatography (Sharpley et al. 2006). It contained 3% phospholipids (w/w) and 0.3 molecules Q_{10} per enzyme molecule. The enzyme did not react with quinones (decylubiquinone) unless phospholipids were present; this reaction was completely rotenone sensitive. In contrast to the classical preparations, it contained only 1 to 1.1 molecules of FMN per enzyme molecule. Its non-heme Fe content was 22–26 Fe atoms per FMN (Sharpley et al. 2006) against 16–18 Fe atoms per FMN for the classical preparations (Hatefi et al. 1962; Ringler et al. 1963; Cremona and Kearney 1964; Lusty et al. 1965; Orme-Johnson et al. 1974; Ohnishi et al. 1981; Paech et al. 1981; Kowal et al. 1986). We will refer to this enzyme as Hirst's NADH dehydrogenase.

The prosthetic groups in Complex I have a redox potential in the range −380 to 0 mV. In contrast to Fe-S proteins from most anaerobic micro-organisms, the Fe-S clusters in Complex I are not destroyed by O_2 because the surrounding protein prevents its access. The most likely places where dioxygen can react are the substrate sites. Hence, FMN-b, FMN-a, the Q-reaction site, as well as ubiquinone itself may be possible targets.

The reactions of dioxygen with Hirst's NADH dehydrogenase have been studied in detail (Kussmaul and Hirst 2006). The enzyme generates superoxide with a rate of ca. 45 nmol.min^{-1}.mg^{-1} in the presence of NADH in aerobic buffer (pH 7.5, 32 °C, measured by the reduction of cytochrome *c*). This rate (ca. 1 s^{-1} as the apparent molecular mass is close to 980 kDa) was not affected by rotenone. The direct generation of H_2O_2 was estimated to be less than 10% of the superoxide production. The redox-potential dependence of the superoxide production in an NADH/NAD$^+$ titration, showed a clear n=2 behaviour and coincided with the expected amount of $FMNH_2$ (see Fig. 5 in (Kussmaul and Hirst 2006)). Because the Fe-S clusters remained reduced in the relevant redox-potential window (−0.3 to −0.4 V), the reduced form of flavin was assigned as the prime target of O_2. Note that the used preparation contained only one flavin, the one reacting with NADH, i.e. FMN-b; hence this is a superoxide-generating site (Fig. 4).

The reaction with O_2 has also been studied with Yoshikawa's Complex I (Ohnishi et al. 2010). Based on EPR studies it was hypothesized that the semiquinone forms of both FMN (i.e. FMN-b) and ubiquinone, induced by reduction with NADH, contribute to the overall formation of $O_2^{\bullet-}$. We note that the actual measured rates (1.3 to 1.76 nmol.min^{1-}.mg^{-1} at pH 7.5 and 32 °C, i.e. ca. 0.022 to 0.029 s^{-1}) were at least one order of magnitude lower than the NADH→O_2 reaction reported for Hirst's NADH dehydrogenase or Hatefi's Complex I (discussed hereafter).

Hatefi reported that Complex I preparations, in which the Nnt was inactivated, showed low rotenone-sensitive NAD(P)H→O_2 activities (Hatefi and Bearden 1976). For

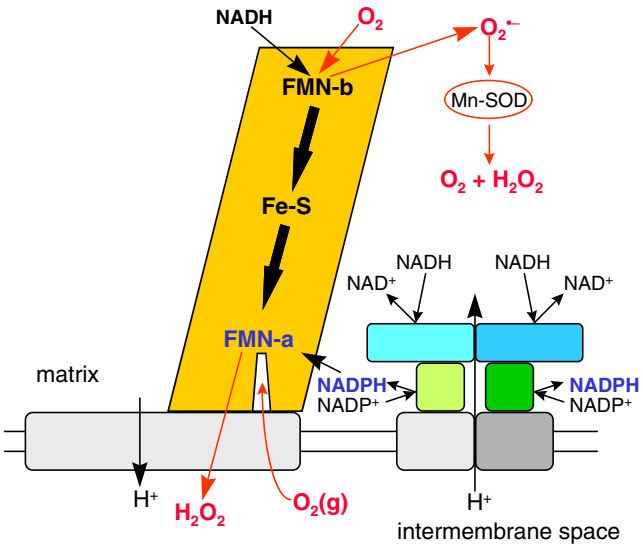

Fig. 5 Schematic representation of the proposed combined actions of bovine Complex I and Nnt (a homodimer) in the mitochondrial inner membrane. When inspecting X-ray structures of the entire Complex I (Efremov et al. 2010) and the EM structures of mitochondrial supercomplexes ("respiratory strings") (Dudkina et al. 2010), it is not inconceivable that Nnt could dock on to the corner of Complex I where NADPH site and FMN-a are situated. The Nnt, steered by the protonmotive force, regulates the NADPH/NADP$^+$ ratio close to the NADPH site. Dioxygen gas reaches FMN-a via the hydrophobic tunnel and reacts with the reduced (very slow) or semiquinone (fast) form. The produced H_2O_2 can easily escape from the enzyme into the intermembrane space and from there to the cytosol. Superoxide formed at FMN-b rapidly diffuses away. It is converted into H_2O_2 and O_2 by (membrane-bound and/or soluble) Mn-SOD. For Complex I the hydrophilic domain is in brown and the membrane domain in grey. The domains of the homodimeric Nnt are in blue (domain I), grey (domain II) and green (domain III)

NADH this activity was 20 nmol.min^{-1}.mg^{-1} in the absence of inhibitor and 7 nmol.min^{-1}.mg^{-1} in its presence. For NADPH the values were 5 and 1 nmol.min^{-1}.mg^{-1}, respectively (pH 7.4 and 22 °C). The rotenone-sensitive activity with NADH (13 nmol.min^{-1}.mg^{-1}) cannot be caused by reduced FMN-b or any of the Fe-S clusters because their rate of reduction is not inhibited by rotenone. Instead, this inhibitor prevents reduction of both FMN-a and Q. Ubiquinol is an unlikely candidate for the reaction with O_2. Its redox potential is thermodynamically unfavourable and QH_2 will not readily react with O_2 (spin forbidden). A reaction with ubisemiquinone is also less likely because no such radical is observed in Hatefi's Complex I reduced with NADH. Instead, it was shown (Sled et al. 1994) that a flavin radical, ascribed by us to FMN-a (see details later on), is always present under these conditions. Hence, we consider the semiquinone of FMN-a as the best candidate for the reaction with O_2 (spin-allowed reaction; thermodynamically favourable).

NADPH does not reduce FMN-b or Q. Instead, it reduces FMN-a to $FMNH_2$. Reaction of $FMNH_2$ with O_2

will be very slow (spin forbidden). Because the reaction of Complex I with NADPH is not sensitive to rotenone (Albracht 2010b), the inhibition of the NADPH→O_2 reaction of the enzyme (Hatefi and Bearden 1976) suggests that it cannot be excluded that rotenone has a second inhibitory effect, e.g. it could interfere with the passage of O_2(g) through the hydrophobic tunnel.

One significant side effect of the reactions between dioxygen and isolated Complex I or NADH dehydrogenases in the presence of NADH is that one of the Fe-S clusters is modified by superoxide. Unlike the enzyme in SMP, Hatefi's Complex I is not stable when reduced with NADH in air. Dramatic changes in the EPR signal of cluster *c* (main EPR line at g=1.94, see (Beinert and Albracht 1982; Albracht 2010b)) can be observed. Within a minute after addition of NADH at room temperature the g=1.94 line starts to decrease while a new signal with g_2=1.97 appears (Hatefi et al. 1962; Kawakita and Ogura 1969; Orme-Johnson et al. 1974). The signals of the other clusters are not affected. This instability is introduced in Hatefi's isolation procedure (Hatefi et al. 1962) at the step where Complex I-III is prepared from Complex I-II-III (Albracht et al. 1977). The presence of dithionite, which effectively consumes all O_2, prevents these NADH-induced changes (Albracht et al. 1977). A g=1.97 line, a marker for the NADH-induced instability, is also present in Hirst's NADH dehydrogenase upon reduction with NADH (Sharpley et al. 2006).

Fragmentation of Singer's NADH dehydrogenase by exposure to NADH in air has been observed long ago (Beinert et al. 1963; Rossi et al. 1965). At 0 °C this resulted in a drastic decrease (60% in 1 h) in the NADH→$K_3Fe(CN)_6$ activity, while the rate of reduction of cytochrome *c* by NADH nearly doubled (to ca. 150 nmol.min^{-1}.mg^{-1} at pH 7.8 and 30 °C). These effects were not influenced by catalase—superoxide dismutase was yet to be discovered (McCord and Fridovich 1969)—but did not take place under N_2. At 20 °C fragmentation was even observed under anaerobic conditions, but then the NADH→$K_3Fe(CN)_6$ and NADH→cytochrome *c* activities did not change. Dithionite did not cause fragmentation. Similar effects have also been observed with Hatefi's Complex I (Kawakita and Ogura 1969). Because the absolute rates of cytochrome *c* reduction (measured aerobically) were only slightly higher than those reported by Hirst and co-workers (Kussmaul and Hirst 2006), we tentatively assume that this reduction was caused by superoxide generated by the enzyme (Fig. 4). Purified bacterial NADH dehydrogenases become also markedly damaged when incubated with NADH in air. In this case the damage is caused by generated H_2O_2 (Berrisford et al. 2008).

The lesson is that the protection of Complex I against the damaging attack by $O_2^{\bullet-}$, formed at FMN-b in the NADH-reduced enzyme in bovine mitochondrial inner membranes, apparently relies on factors that are not present, or that are drastically changed, after purification by classical (Hatefi's Complex I and Singer's NADH dehydrogenase) or modern (Hirst's preparation) means. This may also hold for Complex I preparations from other sources (*E. coli*, *T. thermophilus*), although in that case the main destructive oxygen product is H_2O_2. This lack of protection leads to a variety of damaging reactions of the enzymes by $O_2^{\bullet-}$/H_2O_2. Also other reactions between NADH and purified enzyme performed in air may produce misleading results which may not automatically be extrapolated to more intact systems.

It should be recalled that the respiratory activities of bovine SMP are hardly affected by H_2O_2; for a 10% decrease in the NADH→O_2 activity concentrations of 250 μM or higher were required (Zhang et al. 1990). Likewise, the activities of the Complexes I, III and IV in rat-heart mitochondrial inner membranes were not affected by 50 μM H_2O_2 (Nulton-Persson and Szweda 2001). Hydroxyl radicals and superoxide appeared to be considerably more damaging; a 10% decrease of the overall NADH oxidase activity of bovine SMP was already apparent at concentrations of 7.5 μM and 10 μM, respectively (Zhang et al. 1990).

Production of $O_2^{\bullet-}$ and H_2O_2 by mitochondria and submitochondrial particles

As first reported in 1967 (Hinkle et al. 1967) bovine submitochondrial particles (SMP) can generate H_2O_2 (1.1 nmol.min^{-1}.mg^{-1}) in the presence of dioxygen, NADH and KCN. A similar production (1.2 nmol.min^{-1}.mg^{-1}) was obtained via ATP-induced reverse electron transfer in the presence of succinate and KCN. Rotenone stimulated the first reaction by ca. 30%, but inhibited the second one and so the aspecific reaction with dioxygen was assigned to Complex I.

The difficulty with $O_2^{\bullet-}$/H_2O_2 generation by mitochondria and SMP is that the net productions are dependent on reactions that generate these species and reactions that can remove them. Submitochondrial particles, generally considered as a suspension of inside-out vesicles of inner membranes, are usually obtained by ultrasound. Depending on the power of the ultrasound, the duration of the treatment and the composition of the medium, variable amounts of residual proteins from the matrix and the intermembrane space, as well as membrane-associated, loosely-bound proteins may be present. Hence, SMP suspensions can contain multiple non-protein redox compounds as well as protein-bound redox groups that may be directly or indirectly reducible with NADH and then react with O_2. In addition, the presence of contaminants like

Cu,Zn-SOD (from the intermembrane space (Okado-Matsumoto and Fridovich 2001), cyanide sensitive) as well as Mn-SOD (soluble in the matrix as well as bound to the inner membrane (Okado-Matsumoto and Fridovich 2001), cyanide insensitive) make the interpretation of $O_2^{\bullet-}$ and H_2O_2 generation by SMP not straightforward. It should also be kept in mind, that the relative content of mitochondrial outer membranes of SMP obtained by ultrasound is the same as that in mitochondrial preparations (Albracht and Heidrich 1975). For a proper separation of inner and outer membranes a special procedure is required (see. e.g. (Heidrich et al. 1978)). The variable quality of the SMP preparations is presumably one of the main reasons that reports on $O_2^{\bullet-}/H_2O_2$ production and the effect of inhibitors are confusing and often contradictory (summarized e.g. in (Andreyev et al. 2005; Lambert et al. 2008a; Murphy 2009; Brand 2010; Murphy et al. 2011)). The recent study of Hirst and co-workers (Pryde and Hirst 2011) on the $O_2^{\bullet-}/H_2O_2$ production of bovine SMP is no exception. Although not mentioned, the results confirmed and extended data from 1988 (Krishnamoorthy and Hinkle 1988). Reduced FMN-b was proposed as the only reaction site for O_2 and the rate of $O_2^{\bullet-}/H_2O_2$ production by energy-induced reverse electrons transfer with succinate was found to be considerably smaller than the NADH-induced one (Pryde and Hirst 2011). These results with SMP sharply contradict data obtained with rat-muscle mitochondria (Lambert and Brand 2004a, b; Lambert et al. 2008a, b). We note that two steps in the preparation procedure of the SMP (Pryde and Hirst 2011), i.e. the treatment of mitochondria at pH 9 for ca. 30 min, and an incubation of the SMP with 1 mM NADH for 60 min, may lead to partial (reversible) release of FMN from Complex I as demonstrated by Vinogradov and co-workers (Gostimskaya et al. 2007). Reduction of the *R. eutropha* soluble NAD^+-reducing [NiFe]-hydrogenase by NADH at pH 8 results in the specific rapid (reversible) release of FMN-a, whereas FMN-b remains firmly bound (Van der Linden et al. 2004).

It cannot be ruled out that ultrasound itself may cause subtle mechanically- and/or thermally-induced changes in a large membrane-bound enzyme like Complex I, especially when being part of "respiratory strings" (Dudkina et al. 2010). Acoustic cavitation produced by ultrasound can lead to local hot spots with very high temperatures (5,000 °C) and pressures (500 bar) resulting in the decomposition of water into highly reactive hydrogen atoms and hydroxyl radicals (Suslick 1990; Suslick and Flannigan 2008). In the biochemical context, the reduction of ferricytochrome *c* in water by radicals, notably superoxide, created by ultrasound was already reported in 1972 (Lippitt et al. 1972). The structure of the inner-mitochondrial membrane is certainly affected by ultrasound: the membrane becomes more leaky to protons the more powerful the ultrasonic treatment.

Even during the routine isolation of bovine mitochondria considerable mechanical forces, e.g. the sheering forces in a Potter-Elvehjem homogenizer or those in a Waring Blendor, are applied to free the mitochondria from tissue cells. In addition, the use of mitochondria adds a number of additional complications for the study of $O_2^{\bullet-}/H_2O_2$ generation (Andreyev et al. 2005; Lambert et al. 2008a; Murphy 2009; Brand 2010; Murphy et al. 2011). The study of cell cultures may best approach the in vivo situation, but the techniques for $O_2^{\bullet-}$ and H_2O_2 detection are more demanding (Forkink et al. 2010; Murphy et al. 2011).

In contrast to Complex I, the other respiratory complexes are thought to play a minor role in $O_2^{\bullet-}/H_2O_2$ production. Succinate:ubiquinone oxidoreductase (Complex II) does not noticeably react with O_2. For Complex III it has been demonstrated that in the presence of the specific inhibitor antimycin A, but not in its absence, it can produce H_2O_2 and possibly also $O_2^{\bullet-}$ (Jensen 1966; Andreyev et al. 2005; Murphy 2009). Complex IV reduces O_2 to two molecules of H_2O in a reaction involving four electrons. This complex produces no apparent oxygen by-products. Hence, Complex I is considered to be the main producer of $O_2^{\bullet-}/H_2O_2$ in mammalian mitochondrial inner membranes.

Influence of reactive oxygen species, in particular H_2O_2, on the cell

It is generally accepted that the H_2O_2 concentration in mammalian cells must be carefully kept within certain limits. A high concentration (>3 μM) will lead to direct destruction of cells (necrosis). Intermediate H_2O_2 concentrations (1 to 3 μM) will trigger the mitochondria-dependent process of natural cell death (apoptosis) (Cadenas 2004), while still lower concentrations may just trigger non-specific ("bulk") autophagy or the specific autophagy of damaged cell organelles (e.g. of mitochondria: mitophagy) (Scherz-Shouval et al. 2007; Kim et al. 2007; Semenza 2008a, b; Chen and Gibson 2008; Meijer and Codogno 2009; Chen et al. 2009; Terman et al. 2010). Numerous studies indicate that the mitochondrial H_2O_2 generation is the trigger for these processes (reviewed by (Murphy 2009)). Some recent results suggest that mitochondrial superoxide could be the major trigger of autophagy during starvation (Chen et al. 2009). We note that the mentioned H_2O_2 concentrations (up to 3 μM) are two orders of magnitude lower than those required to affect the NADH→O_2 activity of SMP by 10% (Zhang et al. 1990).

A low H_2O_2 production may enable the cell to evade the normal H_2O_2-regulated turnover cycles of cells, but to keep autophagy going. In healthy tissue this may lead to long-lived cells (Terman et al. 2010). As apparent from the study of Bonnet et al. (Bonnet et al. 2007) also cancer cells

apparently suppress mitochondria-generated H_2O_2 levels to achieve a long life time. In this context, and as indicated above, it is important to keep in mind that the elevated level of HIF-1 in (hypoxic) tumours upregulates proteins involved in mitophagy and downregulates mitochondrial biogenesis. On a longer time scale this can result in a (greatly) decreased mitochondrial density (Pedersen 1978; Luciaková and Kuzela 1992; Zhang et al. 2008) and thus adds to the decrease of their contribution to the cellular H_2O_2 production and mitochondria-induced apoptosis. It is instructive to recall that rat liver contains ca. 2500 mitochondria per cell (Estabrook and Holowinsky 1961), presumably as part of mitochondrial reticula (Westermann 2010).

Role of Nnt in oxidative stress

NADPH produced by Nnt was generally thought to contribute to the NADPH pool in the matrix (Rydström 2006a, b). This pool can be used for the reduction of mitochondrial GSSG to GSH (by glutathione reductase) and for reduction of several mitochondrial redoxins, e.g. thioredoxin (by NADPH-reduced thioredoxin reductase), peroxiredoxin (by thioredoxin) and glutaredoxin (by GSH-reduced thioredoxin reductase). GSH is the main electron donor for the reduction of mitochondrial H_2O_2 (by glutathione peroxidase); for overviews see (Cadenas 2004; Andreyev et al. 2005; Rydström 2006a; Muller et al. 2007; Murphy 2009). In mammalian heart and skeletal muscle the NADPH-producing capacity of the mitochondrial IDH2 is potentially greater than that of Nnt; therefore, the specific physiological role of Nnt in bovine heart has not been well understood (Hoek and Rydström 1988; Jo et al. 2001; Pedersen et al. 2008). It should be kept in mind, however, that the comparison between the activities, determined as maximal initial activities, did not take into account that Nnt, because of its linkage to the Δp, can drive the mitochondrial NADPH/$NADP^+$ ratio to much higher values than IDH2 can. Of course, mitochondrial NADPH is also essential for a number of biosynthetic reactions (Hoek and Rydström 1988; Hatefi and Yamaguchi 1996; Bizouarn et al. 2000).

In vivo effects of Nnt deficiency

Experiments with *Caenorhabditis elegans* with a knockout of Nnt revealed for the first time that Nnt is important in the defence against mitochondrial oxidative stress (Arkblad et al. 2005). It was found that there was an increased sensitivity towards $O_2^{\bullet-}$ (created in mitochondria by addition of methyl viologen). In addition the GSH/GSSG ratio (in lysates) was drastically decreased from 56 in the wild type to 12 in the mutants, a decrease of 80%. If the mitochondrial and cytosolic pools of glutathione were entirely separate, an oxidation of the mitochondrial GSH would not be expected to decrease cellular GSH by more than 10–15%, being the mitochondrial GSH+GSSG content in eukaryotic cells, e.g., hepatocytes. Hence, it was concluded that there might be some kind of communication between the redox states of the glutathione pools in the mitochondrial and cytosolic compartments. The isocitrate-2-oxoglutarate-NADPH shuttle may be responsible for such communication (Papa 1969). An additional possibility, inspired by our hypothesis, is that the specific H_2O_2 production by FMN-a in Complex I is no longer attenuated by Nnt-generated NADPH. The H_2O_2 can escape into the cytosol and contributes to the decrease of the cytosolic GSH/GSSH ratio.

Additional experimental evidence for a specific role of Nnt in the suppression of H_2O_2 came from experiments with mice deficient in Nnt. In 2005 a direct link between Nnt and a metabolic defect (glucose intolerance reminiscent of human type 2 diabetes (Jitrapakdee et al. 2010)) was discovered in C57BL/6J mice with an inactive Nnt (Toye et al. 2005). It was found that the release of insulin induced by high glucose concentrations was strongly diminished when compared to insulin release in other mouse strains. The C57BL/6J mice have a mutation in the *NNT* gene, resulting in an inactive Nnt. Apparently, this prevented glucose from closing the K^+_{ATP} channel in the plasma membrane and so from opening the voltage-gated Ca^{2+} channel in the pancreatic β-cells, resulting in impaired insulin release. Silencing of the *NNT* gene in an insulin-secreting cell line by siRNA confirmed this. In addition it was found that the $O_2^{\bullet-}/H_2O_2$ production increased three-fold relative to the control (Freeman et al. 2006a, b, c). The defects in the C57BL/6J mice could be rescued by transgenic expression of the entire *NNT* gene (Freeman et al. 2006c), whereas increased levels of Nnt in DBA/2 mice (a strain with a normal Nnt activity) led to hypersecretion of insulin in response to glucose challenge (Aston-Mourney et al. 2007).

It was hypothesized that the increased $O_2^{\bullet-}/H_2O_2$ levels in Nnt-deficient mice, induced by a glucose-induced Δp, would stimulate the action of UCP2 (uncoupling protein 2) in the mitochondrial inner membrane. In turn, this would lead to a dissipation of Δp (whereby the $O_2^{\bullet-}/H_2O_2$ production would decrease again), to decreasing ATP levels and hence to a decrease in insulin secretion. (Freeman et al. 2006a, b). However, a knockout of the UCP2 gene had essentially no effect (Parker et al. 2009), suggesting that the glucose intolerance in the C57BL/6J mice does not involve UCP2 but some type of oxidative stress.

Our hypothesis would predict that inactivation of the Nnt will lead to an increased level of H_2O_2 generated by FMN-a in Complex I. In addition, the redox power of the mitochondrial NADPH pool will decrease. The effects will

weaken the power of the cytosolic as well as of the mitochondrial H_2O_2-detoxifying systems. This contributes to the oxidative stress of the cell, followed by oxidative damage, diminished ATP synthesis and so a lower insulin secretion.

C57BL/6J mice show an increased sensitivity to $O_2^{\bullet-}$/H_2O_2, especially in the absence of mitochondrial Mn-SOD (SOD2). A deficiency of both Nnt and Mn-SOD resulted in mice barely surviving 1–2 days (Huang et al. 1999, 2006). In the light of our hypothesis, this would mean that (i) $O_2^{\bullet-}$ generated at FMN-b will have a much longer life time and will cripple the citric-acid cycle by inactivation of aconitase; (ii) H_2O_2 generation at FMN-a will no longer be attenuated resulting in the effects discussed above. C57BL/6J mice where one copy of the *NNT* gene had been re-introduced showed improved cardiovascular functions, i.e. they were more 'normal' than other Nnt-containing mice. However, postnatal survival was not supported. (Kim et al. 2010).

An experimental link between the action of Nnt and cancer

It has been noticed, that the occurrence of spontaneous as well as some types of chemically induced cancers is much lower in C57BL/6J mice than in other mouse strains. Pre-neoplastic lesions and tumours are considerably less common in C57BL/6J than in e.g. C3H/He mice. This was explained by assuming that C3H/He, in contrast to C57BL/6J mice, are genetically predisposed to a high susceptibility to, especially, hepatocarcinogenesis (Bursch et al. 2005). This discrepancy was apparently not dependent on differences in apoptotic activities, but rather on rates of cell division; thus, C57BL/6J mice show a lower rate of cancer cell growth (Bursch et al. 2005). Colorectal tumourigenesis is also less frequent in C57BL/6J mice than in C57BL/6N mice (Diwan and Blackman 1980). Our hypothesis would predict that the absence of Nnt activity will lead to higher H_2O_2 levels. This is analogous to the situation in DCA-treated cancer cells; also in that case a decrease in cell proliferation was observed (Bonnet et al. 2007; Michelakis et al. 2010). In rat liver, apoptosis seems to play a more dominant role in the prevention of tumour formation (Bursch et al. 2005).

Increased $O_2^{\bullet-}$/H_2O_2 generation in heart cells with inhibited Nnt

Inhibition of Nnt with NBD-chloride (4-chloro-7-nitrobenzo-2-oxa-1,3-diazole) in isolated heart cells resulted in an increase of mitochondrial $O_2^{\bullet-}$/H_2O_2 production. The inhibition also contributed to the opening of the innermembrane anion channel (IMAC) and the mitochondrial permeability transition pore (MPT) through a decreased cellular GSH/GSSG ratio (Aon et al. 2007). We note that the phenomena could also be caused by the lack of attenuation of the H_2O_2 production at FMN-a.

Hypothesis in detail

A potential regulatory role for NADPH in the H_2O_2 production by bovine Complex I

The solvent-accessible FMN-b is the site where dissolved dioxygen reacts with $FMNH_2$ resulting in superoxide formation (turnover rate with excess NADH ca. 1 s^{-1}) (Kussmaul and Hirst 2006; Berrisford and Sazanov 2009; Hirst 2010). The $O_2^{\bullet-}$ anion can rapidly escape to the bulk (matrix) aqueous phase. Its detoxification is the task of the Mn-SOD. This enzyme occurs in two forms, a soluble form in the matrix and a innermembrane-bound form (Okado-Matsumoto and Fridovich 2001). The precise binding site in the membrane is not known. It cannot be excluded that it would bind to Complex I close to the site where superoxide escapes after being formed at reduced FMN-b. If not taken care off, $O_2^{\bullet-}$ will rapidly bring the citric-acid cycle to a halt by inactivating aconitase.

FMN-a can be reduced in two ways, i.e. indirectly by electrons from NADH or directly by hydride transfer from NADPH (Fig. 4). Electrons from NADH reach FMN-a via the chain of Fe-S clusters; hence, the initial reduction via this route is a one-electron step. The effective redox power of the electrons reaching FMN-a is considerably lower than that of the NADH/NAD^+ couple. Three redox states of FMN-a may be expected: FMN, $FMNH^{\bullet}$ and $FMNH_2$. In redox titrations performed with Hatefi's Complex I (Sled et al. 1994) in the presence of mediating redox dyes, a bell-shaped curve composed of two $n=1$ reactions was observed for a flavosemiquinone radical EPR signal (linewidth 2.4 mT, midpoint potentials −336 mV and −415 mV at pH 7.5). A maximal semiquinone concentration of 0.1 spin per FMN was obtained at −368 mV. Piericidin A or rotenone did not affect the titration. The radical showed a strong spin-spin interaction with a nearby Fe-S cluster having a g_3 EPR line at 1.86. As a result its spin relaxation was greatly enhanced and it was not saturated by a microwave power of 100 mW at 169 K. A titration with NADH/NAD^+ and AcPyADH/$AcPyAD^+$ (AcPyADH, reduced 3-acetylpyridine adenine dinucleotide), both obligatory $n=2$ redox couples, at pH 8.2 in the absence of redox mediators gave very different results (see Fig. 8 in (Sled et al. 1994)). A maximal semiquinone signal (0.035 spins per FMN, linewidth 1.7 mT) was now observed at −310 mV. With mediators the signal peaked at −390 mV (0.11 spins per FMN) at the same pH. In contrast to the titrations with mediators, the signal did not disappear completely at the

lowest potentials (−440 mV and below) obtained with NADH/NAD^+; ca. 0.02 spins per FMN persisted. The radical's relaxation properties and its spin-spin interaction with the g_3=1.86 signal were the same as observed in the titration in the presence of mediators.

At the time, the authors (Sled et al. 1994) assumed that Complex I contained only one FMN group, and hence explanations for the observed phenomena were based on that. We suggest that both flavins may have equally contributed to the flavosemiquinone signal in potentiometric titrations in the presence of mediators. However, in the pyridine-nucleotide titrations the contributions are expected to differ. It is questionable whether FMN-b will contribute because the nucleotides are obligatory n=2 redox agents. In contrast, FMN-a receives electrons via the Fe-S clusters (n=1 redox groups). Hence, we assume that in that case the observed flavosemiquinone radical signal was mainly due to FMN-a. This explains why even the lowest redox potentials, obtained with NADH/NAD^+, could not eliminate the radical signal. The expected redox behaviour of FMN-b in the presence of NADH/NAD^+, i.e. an $FMNH_2$/FMN equilibrium without the flavosemiquinone form, is in agreement with the observed superoxide generation of Hirst's NADH dehydrogenase (which contains only FMN-b) with NADH/NAD^+ (Kussmaul and Hirst 2006). We also note that in contrast to Hatefi's Complex I (Sled et al. 1994), there was no hint of a flavosemiquinone EPR signal in Hirst's NADH dehydrogenase at either −0.3 V or −0.4 V, even in the 40 K spectra (Kussmaul and Hirst 2006). This is in agreement with our explanation that the NADH-induced flavosemiquinone radical EPR signal in Hatefi's Complex I is caused by FMN-a. Our interpretation also suggests that the spin-spin interaction between the flavosemiquinone radical and the reduced Fe-S cluster with g_3=1.86 observed by Ohnishi and co-workers (Salerno et al. 1977; Ingledew and Ohnishi 1980; Sled et al. 1994) is one between FMN-a and cluster *h*. This is consistent with the observed rapid reduction of cluster *h* (g_3=1.86) by NADPH (Albracht 2010b).

The direct redox reaction of FMN-a with the NADPH/$NADP^+$ couple will result in an $FMNH_2$/FMN equilibrium. However, in the in vivo situation FMN-a will receive reducing equivalents both from NADH, via the chain of Fe-S clusters, and from NADPH. Hence, there will be three different reactions. Two are induced by the NADH/NAD^+ couple:

$$FMN + e^- + H^+ \leftrightarrow FMNH^\bullet$$

$$FMNH^\bullet + e^- + H^+ \leftrightarrow FMNH_2$$

The kinetics of the two forward reactions are rotenone sensitive. Also electrons coming in via energy-induced reverse electron transfer from the Q-pool can contribute here (rotenone sensitive). The third reaction is ruled by the NADPH/$NADP^+$ couple (kinetics insensitive to rotenone):

$$FMN + 2e^- + 2H^+ \leftrightarrow FMNH_2$$

The concentration of the flavosemiquinone, the form that can rapidly react with dioxygen to form $O_2^{\bullet-}$ (a spin-allowed reaction), is thus dependent on both the NADH/NAD^+ and the NADPH/$NADP^+$ couples. At high NADPH/$NADP^+$ ratios, the level of $FMNH_2$ will be maximized. The reaction of $FMNH_2$ with dioxygen is spin forbidden. For free flavin in aqueous solution the rate of reaction of $FMNH^\bullet$ with O_2 (second order rate constant ca. 10^4 $M^{-1}.s^{-1}$) is three orders of magnitude faster than that of the reaction with $FMNH_2$ (Bruice 1982; Anderson 1982; Lind and Merenyi 1990). The superoxide anion formed at FMN-a cannot escape through the hydrophobic tunnel (caging) and so H_2O_2 is formed by spontaneous dismutation (second order rate constant ca. 10^7 $M^{-1}.s^{-1}$), as well as by further reduction via regenerated $FMNH^\bullet$. The hydrogen peroxide then leaves the enzyme at a site close to the inner membrane. Thus, increasing NADPH/$NADP^+$ ratio's will attenuate the rate of H_2O_2 generation at FMN-a independently of the NADH/NAD^+ ratio. Under turnover conditions rotenone will inhibit the NADH-induced flavosemiquinone formation at FMN-a, and so it will minimize the H_2O_2 production. The observed inhibition in cancer cells of the DCA-induced H_2O_2 production by micro-injected intracellular catalase (Bonnet et al. 2007) suggests that most of the hydrogen peroxide can escape into the intermembrane space and from there to the cytoplasm. This suggests that potential target sites for this signal molecule may be situated (also) outside the matrix. Although it is generally assumed that H_2O_2 can pass freely through biological membranes, recent studies indicate that specific aquaporins may be involved (Miller et al. 2010).

Co-operation between Complex I and transhydrogenase in the control of H_2O_2

The major generators of NADPH in mammalian mitochondria are Nnt, the mitochondrial $NADP^+$-linked isocitrate dehydrogenase (iso-enzyme 2, IDH2 (Pollard and Ratcliffe 2009)), malic enzyme (see e.g. (Rydström 2006a)) and perhaps glutamate dehydrogenase (Meijer and Codogno 2009). The NADH site of Complex I sticks out well (ca. 130 Å) into the matrix space (Efremov et al. 2010). The proposed reaction site for Complex I with NADPH is, however, very close to the membrane. It has consistently been reported that the Nnt in bovine-heart SMP partly co-purifies with Complex I in the Hatefi procedure (Ragan and Widger 1975; Hatefi and Bearden 1976; Ragan 1976; Finel et al. 1992). Hence it is conceivable that the Nnt, a membrane-bound enzyme, is weakly bound to Complex I

in the mitochondrial inner membrane. The Complex I content of bovine-heart SMP is 0.06 nmol.mg^{-1} (Albracht 2010b). From the reverse (NADPH generation) Nnt activity of SMP (ca. 0.2 μmol/min/mg), the activity of purified Nnt (ca. 15 μmol/min/mg) and the molecular mass (218 kDa) (Persson et al. 1984), it follows that SMP contain ca. 0.06 nmol Nnt per mg of protein. Thus, the concentrations of the two enzymes in bovine-heart SMP are about the same.

The structural information on Nnt (Bizouarn et al. 2000; Cotton et al. 2001; Jackson 2003; Pedersen et al. 2008) shows that its NADPH-producing site is close to the membrane surface, as was already predicted from inhibitor studies in 1972 (Rydström 1972). An association between the two enzymes could rule the NADPH/NADP$^+$ ratio in the vicinity of the NADPH site of Complex I (Fig. 5). This would enable a rapid and specific control mechanism of Complex I-dependent H_2O_2 generation steered by the mitochondrial energy status, the protonmotive force. Excess NADPH will diffuse into the bulk matrix space. Because Nnt is a key NADPH generator in cancer cells, using Nnt inhibitors as pharmaceuticals may help to improve future cancer therapy.

The expression of several of the enzymes involved mitochondrial $O_2^{\bullet-}/H_2O_2$ detoxification, e.g. Mn-SOD and glutathione peroxidase, is stimulated by H_2O_2 (Jo et al. 2001). These biosynthetic processes are much slower than the proposed attenuation by NADPH/NADP$^+$ of H_2O_2 generation by Complex I. We therefore consider these scavenging systems as more general (global) ones. They may even be unable to sufficiently cope with H_2O_2 produced by Complex I close to the inner membrane, especially when, as indicated by experiments of Michelakis and co-workers (Bonnet et al. 2007), the rotenone-sensitive H_2O_2 produced in DCA-treated cancer cells can easily escape into the cytoplasm. Rather, they will deal with H_2O_2 produced elsewhere in matrix. We note that the H_2O_2-detoxifying systems are all involved in the indiscriminate *removal* of this oxygen product. In contrast, our hypothesis predicts that the reaction of the NADPH/NADP$^+$ couple with Complex I may result in an *increase* or *decrease* of the H_2O_2 levels specific for signalling in apoptosis and autophagy, depending on the mitochondrial energetic conditions.

The hypothesis is in agreement with the results and conclusions of Lambert and Brand (Lambert and Brand 2004a, b; Lambert et al. 2008a, b) that Complex I in rat-muscle mitochondria produces $O_2^{\bullet-}/H_2O_2$ at two sites. The minor site was proposed to be the FMN reacting with NADH (i.e. FMN-b). The major site was thought to be in the region of the Q-binding site, possibly ubisemiquinone itself (Lambert and Brand 2004b). Our hypothesis predicts that this second site is FMN-a.

References

Ackrell BAC, Kearney EB, Singer TP (1977) Effect of membrane environment on succinate dehydrogenase activity. J Biol Chem 252:1582–1588

Albracht SPJ (2010a) The reaction of NADPH with bovine mitochondrial NADH:ubiquinone oxidoreductase revisited: II. Comparison of the proposed working hypothesis with literature data. J Bioenerg Biomembr 42:279–292

Albracht SPJ (2010b) The reaction of NADPH with bovine mitochondrial NADH: ubiquinone oxidoreductase revisited: I. Proposed consequences for electron transfer in the enzyme. J Bioenerg Biomembr 42:261–278

Albracht SPJ, Heidrich HG (1975) Beef-heart submitochondrial particles: a mixture of mitochondrial inner and outer membranes. Biochim Biophys Acta 376:231–236

Albracht SPJ, Hedderich R (2000) Learning from hydrogenases: location of a proton pump and of a second FMN in bovine NADH-ubiquinone oxidoreductase (Complex I). FEBS Lett 485:1–6

Albracht SPJ, Dooijewaard G, Leeuwerik FJ, Swol BV (1977) EPR signals of NADH: Q oxidoreductase. Shape and intensity. Biochim Biophys Acta 459:300–317

Albracht SPJ, Van der Linden E, Faber BW (2003) Quantitative amino acid analysis of bovine NADH: ubiquinone oxidoreductase (Complex I) and related enzymes. Consequences for the number of prosthetic groups. Biochim Biophys Acta 1557:41–49

Anderson RF (1982) In: Massey V, Williams CH (eds) Flavins and flavoproteins: flavin-oxygen complex formed on the reaction of superoxide ions with flavosemiquinone radicals. Elsevier North-Holland, Inc., New York, pp 278–283

Andreyev AY, Kushnareva YE, Starkov AA (2005) Mitochondrial metabolism of reactive oxygen species. Biochemistry (Moscow) 70:200–214

Aon MA, Cortassa S, Maack C, O'Rourke B (2007) Sequential opening of mitochondrial ion channels as a function of glutathione redox thiol status. J Biol Chem 282:21889–21900

Arkblad EL, Tuck S, Pestov NB, Dmitriev RI, Kostina MB, Stenvall J, Tranberg M, Rydström J (2005) A *Caenorhabditis elegans* mutant lacking functional nicotinamide nucleotide transhydrogenase displays increased sensitivity to oxidative stress. Free Radic Biol Med 38:1518–1525

Armstrong FA, Albracht SPJ (2005) [NiFe]-hydrogenases: spectroscopic and electrochemical definition of reactions and intermediates. Phil Trans R Soc A 363:937–954

Aston-Mourney K, Wong N, Kebede M, Zraika S, Balmer L, McMahon JM, Fam BC, Favaloro J, Proietto J, Morahan G, Andrikopoulos S (2007) Increased nicotinamide nucleotide transhydrogenase levels predispose to insulin hypersecretion in a mouse strain susceptible to diabetes. Diabetologia 50:2467–2485

Bakker PT, Albracht SPJ (1986) Evidence for two independent pathways of electron transfer in mitochondrial NADH:Q oxidoreductase. I. Pre-steady-state kinetics with NADPH. Biochim Biophys Acta 850:413–422

Beinert H, Albracht SPJ (1982) New insights, ideas and unanswered questions concerning iron-sulfur clusters in mitochondria. Biochim Biophys Acta 683:245–277

Beinert H, Palmer G, Cremona T, Singer TP (1963) Correlation of enzymatic activity and the appearance of the EPR signal at g=1.94 in NADH dehydrogenase and its thermal breakdown products. Biochem Biophys Res Commun 12:432–438

Beinert H, Kennedy MC, Stout CD (1996) Aconitase as iron-sulfur protein, enzyme, and iron-regulatory protein. Chem Rev 96:2335–2373

Belevich G, Euro L, Wikström M, Verkhovskaya M (2007) Role of the conserved Arginine 274 and Histidine 224 and 228 residues in the NuoCD subunit of complex I from *Escherichia coli*. Biochemistry 46:526–533

Berrisford JM, Sazanov LA (2009) Structural basis for the mechanism of respiratory complex I. J Biol Chem 284:29773–29783

Berrisford JM, Thompson CJ, Sazanov LA (2008) Chemical and NADH-induced, ROS-dependent, cross-linking between subunits of complex I from *Escherichia coli* and *Thermus thermophilus*. Biochemistry 47:10262–10270

Bizouarn T, Meuller J, Axelsson M, Rydström J (2000) The transmembrane domain and the proton channel in proton-pumping transhydrogenases. Biochim Biophys Acta 1459:284–290

Bonnet S, Archer SL, Allalunis-Turner J, Haromy A, Beaulieu C, Thompson R, Lee CT, Lopaschuk GD, Puttagunta L, Bonnet S, Harry G, Hashimoto K, Porter CJ, Andrade MA, Thebaud B, Michelakis ED (2007) A mitochondria-K^+ channel axis is suppressed in cancer and its normalization promotes apoptosis and inhibits cancer growth. Cancer Cell 11:37–51

Borst P, Rottenberg S (2004) Cancer cell death by programmed necrosis? Drug Resist Update 7:321–324

Brand MD (2010) The sites and topology of mitochondrial superoxide production. Exp Gerontol 45:466–472

Bruice TC (1982) In: Massey V, Williams CH (eds) Flavins and flavoproteins: a progress report on studies of the activation of molecular oxygen by dihydroflavins. Elsevier North-Holland, Inc., New York, pp 265–277

Bursch W, Chabicovsky M, Wastl U, Grasl-Kraupp B, Bukowska K, Taper H, Schulte-Hermann R (2005) Apoptosis in stages of mouse hepatocarcinogenesis: failure to counterbalance cell proliferation and to account for strain differences in tumor susceptibility. Toxicol Sci 65:515–529

Cadenas E (2004) Mitochondrial free radical production and cell signaling. Mol Aspects Med 25:17–26

Cao W, Yacoub S, Shiverick KT, Namiki K, Sakai Y, Porvasnik S, Urbanek C, Rosser CJ (2008) Dichloroacetate (DCA) sensitizes both wild-type and over expressing *Bcl-2* prostate cancer cells in vitro to radiation. Prostate 68:1223–1231

Carroll J, Fearnley IM, Skehel JM, Shannon RJ, Hirst J, Walker JE (2006) Bovine complex I is a complex of 45 different subunits. J Biol Chem 281:32724–32727

Chen LB (1988) Mitochondrial membrane potential in living cells. Annu Rev Cell Biol 4:155–181

Chen Y, Gibson SB (2008) Is mitochondrial generation of reactive oxygen species a trigger for autophagy? Autophagy 4:246–248

Chen Y, Azad MB, Gibson SB (2009) Superoxide is the major reactive oxygen species regulating autophagy. Cell Death Differ 16:1040–1052

Chin L, Gray JW (2008) Translating insights from the cancer genome into clinical practice. Nature 452:553–563

Cittadini A, Galeotti T, Terranova T (1971) The effect of pyruvate on cyanide-inhibited respiration in intact ascites tumor cells. Experientia 27:633–635

Cotton NPJ, White SA, Peake SJ, McSweeney S, Jackson JB (2001) The crystal structure of an asymmetric complex of the two nucleotide binding components of proton-translocating transhydrogenase. Structure 9:165–176

Cremona T, Kearney EB (1964) Studies on the respiratory chain-linked NADH dehydrogenase. VI. Further purification and properties of the enzyme from beef heart. J Biol Chem 239:2328–2334

De Jong L, Kemp A (1984) Stoicheiometry and kinetics of the prolyl 4-hydroxylase partial reaction. Biochim Biophys Acta 787:105–111

De Jong L, Albracht SPJ, Kemp A (1982) Prolyl 4-hydroxylase activity in relation to the oxidation state of enzyme-bound iron. The role of ascorbate in peptidyl proline hydroxylation. Biochim Biophys Acta 704:326–332

Diwan BA, Blackman KE (1980) Differential susceptibility of 3 sublines of C57BL/6 mice to the induction of colorectal tumors by 1,2-dimethylhydrazine. Cancer Lett 9:111–115

Djafarzadeh R, Kerscher S, Zwicker K, Radermacher M, Lindahl M, Schägger H, Brandt U (2000) Biophysical and structural characterization of proton-translocating NADH-dehydrogenase (complex I) from the strictly aerobic yeast *Yarrowia lipolytica*. Biochim Biophys Acta 1459:230–238

Dooijewaard G, Slater EC (1976) Steady-state kinetics of high molecular weight (type-I) NADH dehydrogenase. Biochim Biophys Acta 440:1–15

Dudkina NV, Kouril R, Peters K, Braun H-P, Boekema EJ (2010) Structure and function of mitochondrial supercomplexes. Biochim Biophys Acta 1797:664–670

Efremov RG, Baradaran R, Sazanov LA (2010) The architecture of respiratory complex I. Nature 465:441–445

Ellyard PW, San Pietro A (1969) The Warburg effect in a chloroplast-free preparation from *Euglena gracilis*. Plant Physiol 44:1679–1683

Ernster L, Dallner G, Azzone GF (1963) Differential effects of rotenone and amytal on mitochondrial electron and energy transfer. J Biol Chem 238:1124–1131

Estabrook RW, Holowinsky A (1961) Studies on the content and organization of the respiratory enzymes of mitochondria. J Biophys Biochem Cytol 9:19–28

Eytan GD, Carlenor E, Rydström J (1990) Energy-linked transhydrogenase. Effects of valinomycin and nigericn on the ATP-driven transhydrogenase reaction catalyzed by reconstituted transhydrogenase-ATPase vesicles. J Biol Chem 265:12949–12954

Fantin VR, St-Pierre J, Leder P (2006) Attenuation of LDH-A expression uncovers a link between glycolysis, mitochondrial physiology, and tumor maintenance. Cancer Cell 9:425–434

Fearnley IM, Walker JE (1992) Conservation of sequences of subunits of mitochondrial complex I and their relationships with other proteins. Biochim Biophys Acta 1140:105–134

Finel M, Skehel JM, Albracht SPJ, Fearnley IM, Walker JE (1992) Resolution of NADH: ubiquinone oxidoreductase from bovine heart mitochondria into two subcomplexes, one of which contains the redox centers of the enzyme. Biochemistry 31:11425–11434

Finel M, Majander AS, Tyynelä J, De Jong AMP, Albracht SPJ, Wikström M (1994) Isolation and characterisation of subcomplexes of the mitochondrial NADH: ubiquinone oxidoreductase (complex I). Eur J Biochem 226:237–242

Flint DH, Tuminello JF, Emptage MH (1993) The inactivation of Fe-S cluster containing hydro-lyases by superoxide. J Biol Chem 268:22369–22376

Fontecilla-Camps JC, Volbeda A, Cavazza C, Nicolet Y (2007) Structure/function relationships of [NiFe]- and [FeFe]-hydrogenases. Chem Rev 107:4273–4303

Forkink M, Smeitink JAM, Brock R, Willems PHGM, Koopman WJH (2010) Detection and manipulation of mitochondrial reactive oxygen species in mammalian cells. Biochim Biophys Acta 1797:1034–1044

Freeman H, Shimomura K, Cox RD, Ashcroft FM (2006a) Nicotinamide nucleotide transhydrogenase: a link between insulin secretion, glucose metabolism and oxidative stress. Biochem Soc Trans 34:806–810

Freeman H, Shimomura K, Horner E, Cox RD, Ashcroft FM (2006b) Nicotinamide nucleotide transhydrogenase: a key role in insulin secretion. Cell Metab 3:35–45

Freeman HC, Hugill A, Dear NT, Ashcroft FM, Cox RD (2006c) Deletion of nicotinamide nucleotide transhydrogenase. A new quantitive trait locus accounting for glucose intolerance in C57BL/6J mice. Diabetes 55:2153–2156

Galkin AS, Grivennikova VG, Vinogradov AD (1999) $H^+/2e^-$ stoichiometry in NADH-quinone reductase reactions catalyzed by bovine heart submitochondrial particles. FEBS Lett 451:157–161

George SJ, Kurkin S, Thorneley RNF, Albracht SPJ (2004) Reactions of H_2, CO, and O_2 with active [NiFe]-hydrogenase from *Allochromatium vinosum*. A stopped-flow infrared study. Biochemistry 43:6808–6819

Gostimskaya IS, Grivennikova VG, Cecchini G, Vinogradov AD (2007) Reversible dissociation of flavin mononucleotide from the mammalian membrane-bound NADH:ubiquinone oxidoreductase (Complex I). FEBS Lett 581:5803–5806

Grgic L, Zwicker K, Kashani-Poor N, Kerscher S, Brandt U (2004) Functional significance of conserved histidines and arginines in the 49-kDa subunit of mitochondrial complex I. J Biol Chem 279:21193–21199

Grigorieff N (1998) Three-dimensional structure of bovine NADH: ubiquinone oxidoreductase (complex I) at 22 Å in ice. J Mol Biol 277:1033–1046

Guénebaut V, Vincentelli R, Mills D, Weiss H, Leonard KR (1997) Three-dimensional structure of NADH-dehydrogenase from *Neurospora crassa* by electron microscopy and conical tilt reconstruction. J Mol Biol 265:409–418

Guénebaut V, Schlitt A, Weiss H, Leonard K, Friedrich T (1998) Consistent structure between bacterial and mitochondrial NADH: ubiquinone oxidoreductase (Complex I). J Mol Biol 276:105–112

Gutman M, Singer TP, Casida JE (1970) Studies on the respiratory chain-linked reduced nicotinamide adenine dinucleotide dehydrogenase. XVII. Reaction sites of piericidin A and rotenone. J Biol Chem 245:1992–1997

Happe RP, Roseboom W, Pierik AJ, Albracht SPJ, Bagley KA (1997) Biological activation of hydrogen. Nature 385:126

Hatefi Y, Hanstein WG (1973) Interactions of reduced and oxidized triphosphopyridine nucleotides with the electron-transport system of bovine heart mitochondria. Biochemistry 12:3515–3522

Hatefi Y, Bearden AJ (1976) Electron paramagnetic resonance studies on the reduction of the components of complex I and transhydrogenase-inhibited complex I by NADH and NADPH. Biochem Biophys Res Commun 69:1032–1038

Hatefi Y, Yamaguchi M (1996) Nicotinamide nucleotide transhydrogenase: a model for utilization of substrate binding energy for proton translocation. FASEB J 10:444–452

Hatefi Y, Haavik AG, Griffiths DE (1962) Studies on the electron transfer system; XL. Preparation and properties of mitochondrial DPNH-Coenzyme Q reductase. J Biol Chem 237:1667–1680

Heerdt BG, Houston MA, Augenlicht LH (2006) Growth properties of colonic tumor cells are a function of the intrinsic mitochondrial membrane potential. Cancer Res 66:1591–1596

Heidrich HG, Albracht SPJ, Bäckström D (1978) Two iron-sulfur centers in mitochondrial outer membranes from beef heart as prepared by free-flow electrophoresis. FEBS Lett 95:314–318

Hinkle PC, Butow RA, Racker E, Chance B (1967) Partial resolution of the enzymes catalyzing oxidative phosphorylation. XV. Reverse electron transfer in the flavin-cytochrome b region of the respiratory chain of beef heart submitochondrial particles. J Biol Chem 242:5169–5173

Hirst J (2010) Towards the molecular mechanism of respiratory complex I. Biochem J 425:327–339

Hirst J, Carroll J, Fearnley IM, Shannon RJ, Walker JE (2003) The nuclear encoded subunits of complex I from bovine heart mitochondria. Biochim Biophys Acta 1604:135–150

Hoek JB, Rydström J (1988) Physiological roles of nicotinamide nucleotide transhydrogenase. Biochem J 254:1–10

Hofhaus G, Weiss H, Leonard K (1991) Electron microscopic analysis of the peripheral and membrane parts of mitochondrial NADH dehydrogenase (complex I). J Mol Biol 221:1027–1043

Huang T-T, Carlson EJ, Raineri I, Gillespie AM, Kozy H, Epstein CJ (1999) The use of transgenic and mutant mice to study oxygen free radical metabolism. Ann NY Acad Sci 893:95–112

Huang T-T, Naeemuddin M, Elchuri S, Yamaguchi M, Kozy HM, Carlson EJ, Epstein CJ (2006) Genetic modifiers of the phenotype of mice deficient in mitochondrial superoxide dismutase. Hum Mol Genet 15:1187–1194

Hunte C, Zickermann V, Brandt U (2010) Functional modules and structural basis of conformational coupling in mitochondrial complex I. Science 329:448–451

Ingledew WJ, Ohnishi T (1980) An analysis of some thermodynamic properties of iron-sulphur centres in site I of mitochondria. Biochem J 186:111–117

Ivan M, Kondo K, Yang H, Kim W, Valiando J, Ohh M, Salic A, Asara JM, Lane WS, Kaelin WG Jr (2001) HIFα targeted for VHL-mediated destruction by proline hydroxylation: implications for O_2 sensing. Science 292:464–468

Jaakkola P, Mole DR, Tian Y-M, Wilson MI, Gielbert J, Gaskell SJ, Von Kriegsheim A, Hebestreit HF, Mukherji M, Schofield CJ, Maxwell PH, Pugh CW, Ratcliffe PJ (2001) Targeting of HIF-α to the von Hippel- Lindau ubiquitylation complex by O_2-regulated prolyl hydroxylation. Science 468–472.

Jackson JB (2003) Proton translocation by transhydrogenase. FEBS Lett 545:18–24

Jensen PK (1966) Antimycin-insensitive oxidation of succinate and reduced nicotinamide-adenine dinucleotide in electron-transport particles. I. pH dependency and hydrogen peroxide formation. Biochim Biophys Acta 122:157–166

Jiang P, Du W, Wang X, Mancuso A, Gao X, Wu M, Yang X (2011) p53 regulates biosynthesis through direct inactivation of glucose-6-phosphate dehydrogenase. Nat Cell Biol 13:310–316

Jitrapakdee S, Wutthisathapornchai A, Wallace JC, MacDonald MJ (2010) Regulation of insulin secretion: role of mitochondrial signalling. Diabetologia 53:1019–1032

Jo S-H, Son M-K, Koh H-J, Lee S-M, Song I-H, Kim Y-O, Lee Y-S, Jeong K-S, Kim WB, Park J-W, Song BJ, Huh T-L (2001) Control of mitochondrial redox balance and cellular defense against oxidative damage by mitochondrial $NADP^+$-dependent isocitrate dehydrogenase. J Biol Chem 276:16168–16176

Jones S, Zhang X, Parsons DW, Lin JC-H, Leary RJ, Angenendt P, Mankoo P, Carter H, Kamiyama H, Jimeno A, Hong S-M, Fu B, Lin M-T, Calhoun ES, Kamiyama M, Walter K, Nikolskaya T, Nikolsky Y, Hartigan J, Smith DR, Hidalgo M, Leach SD, Klein AP, Jaffee EM, Goggins M, Maitra A, Iacobuzio-Donahue C, Eshleman JR, Kern SE, Hruban RH, Karchin R, Papadopoulos N, Parmigiani G, Vogelstein B, Velculescu VE, Kinzler KW (2008) Core signaling pathways in human pancreatic cancers revealed by global genomic analyses. Science 321:1801–1806

Kaelin WG Jr, Ratcliffe PJ (2008) Oxygen sensing by metazoans: the central role of the HIF hydroxylase pathway. Mol Cell 30:393–402

Kashani-Poor N, Zwicker K, Kerscher S, Brandt U (2001) A central functional role for the 49-kDa subunit within the catalytic core of mitochondrial complex I. J Biol Chem 276:24082–24087

Kato M, Li J, Chuang JL, Chuang DT (2007) Distinct structural mechanisms for inhibition of pyruvate dehydrogenase kinase isoforms by AZD7545, dichloroacetate, and radicicol. Structure 15:992–1004

Kawakita M, Ogura Y (1969) Spectrophotometric and electron spin resonance studies of $NADH_2$-cytochrome *c* reductase complex. J Biochem (Japan) 66:203–211

Kim K, Rodriguez-Enriquez S, Lemasters JL (2007) Selective degradation of mitochondria by mitophagy. Arch Biochem Biophys 462:245–253

Kim A, Chen C-H, Ursell P, Huang T-T (2010) Genetic modifier of mitochondrial superoxide dismutase-deficient mice delays heart failure and prolongs survival. Mamm Genome 21:534–542

Knowles HJ, Raval RR, Harris AL, Ratcliffe PJ (2003) Effect of ascorbate on the activity of hypoxia-inducible factor in cancer cells. Cancer Res 63:1764–1768

Koppenol W, Stanbury DM, Bounds PL (2010) Electrode potentials of partially reduced oxygen species, from dioxygen to water. Free Radic Biol Med 49:317–322

Kowal AT, Morningstar JE, Johnson MK, Ramsay RR, Singer TP (1986) Spectroscopic characterization of the number and type of iron-sulfur clusters in NADH: ubiquinone oxidoreductase. J Biol Chem 261:9239–9245

Krishnamoorthy G, Hinkle PC (1988) Studies on the electron transfer pathway, topography of iron-sulfur centers, and site of coupling in NADH-Q oxidoreductase. J Biol Chem 263:17566–17575

Kuiper C, Molenaar IGM, Dachs GU, Currie MJ, Sykes PH, Vissers MCM (2010) Low ascorbate levels are associated with increased hypoxia-inducible factor-1 activity and an aggressive tumor phenotype in endometrial cancer. Cancer Res 70:5749–5758

Kurkin S, George SJ, Thorneley RNF, Albracht SPJ (2004) Hydrogen-induced activation of the [NiFe]-hydrogenase from *Allochromatium vinosum* as studied by stopped-flow infrared spectroscopy. Biochemistry 43:6820–6831

Kussmaul L, Hirst J (2006) The mechanism of superoxide production by NADH: ubiquinone oxidoreductase (complex I) from bovine heart mitochondria. Proc Natl Acad Sci (USA) 103:7607–7612

Lambert AJ, Brand MD (2004a) Superoxide production by NADH: ubiquinone oxidoreductase (complex I) depends on the pH gradient across the mitochondrial inner membrane. Biochem J 382:511–517

Lambert AJ, Brand MD (2004b) Inhibitors of the quinone-binding site allow rapid superoxide production from mitochondrial NADH: ubiquinone oxidoreductase (complex I). J Biol Chem 279:39414–39420

Lambert AJ, Buckingham JA, Boysen HM, Brand MD (2008a) Diphenyleneiodonium acutely inhibits reactive oxygen species production by mitochondrial complex I during reverse, but not forward electron transport. Biochim Biophys Acta 1777:397–403

Lambert AJ, Buckingham JA, Brand MD (2008b) Dissociation of superoxide production by mitochondrial complex I from NAD(P) H redox state. FEBS Lett 592:1711–1714

Le A, Cooper CR, Gouw AM, Dinavahi R, Maitra A, Deck LM, Royer RE, Vander Jagt DL, Semenza GL, Dang CV (2010) Inhibition of lactate dehydrogenase A induces oxidative stress and inhibits tumor progression. Proc Natl Acad Sci (USA) 107:2037–2042

Leonard K, Haiker H, Weiss H (1987) Three-dimensional structure of NADH: ubiquinone reductase (complex I) from *Neurospora* mitochondria determined by electron microscopy of membrane crystals. J Mol Biol 194:277–286

Li J, Kato M, Chuang DT (2009) Pivotal role of the C-terminal DW-motif in mediating inhibition of pyruvate dehydrogenase kinase 2 by dichloroacetate. J Biol Chem 284:34458–34467

Lind J, Merenyi G (1990) Kinetics and thermodynamics of the autoxidation of reduced flavin mononucleotide (FMN). Photochem Photobiol 51:21–27

Lippitt B, McCord JM, Fridovich I (1972) The sonochemical reduction of cytochrome *c* and its iInhibition by superoxide dismutase. J Biol Chem 247:4668–4690

Lu C-W, Lin S-C, Chen K-F, Lai Y-Y, Tsai S-J (2008) Induction of pyruvate dehydrogenase kinase-3 by hypoxia-inducible factor-1 promotes metabolic switch and drug resistance. J Biol Chem 283:28106–28114

Luciaková K, Kuzela S (1992) Increased steady-state levels of several mitochondrial and nuclear gene transcripts in rat hepatoma with a low content of mitochondria. Eur J Biochem 205:1187–1193

Lusty CJ, Machinist JM, Singer TP (1965) Studies on the respiratory chain-linked NADH dehydrogenase. VII. Labile sulfide groups in the dehydrogenase and in related proteins. J Biol Chem 240:1804–1810

Madhok BM, Yeluri S, Perry SL, Hughes TA, Jayne DG (2010) Dichloroacetate induces apoptosis and cell-cycle arrest in colorectal cancer cells. Br J Canc 102:1746–1752

Mathupala SP, Ko YH, Pedersen PL (2009) Hexokinase-2 bound to mitochondria: cancer's stygian link to the "Warburg effect"and a pivotal target for effective therapy. Semin Cancer Biol 19:17–24

Mathupala SP, Ko YH, Pedersen PL (2010) The pivotal roles of mitochondria in cancer: Warburg and beyond and encouraging prospects for effective therapies. Biochim Biophys Acta 1797:1225–1230

McCord JM, Fridovich I (1969) Superoxide dismutase. An enzymic function for erythrocuprein (hemocuprein). J Biol Chem 244:6049–6055

McCord JM, Fridovich I (1978) The biology and pathology of oxygen radicals. Ann Intern Med 89:122–127

Meijer AJ, Codogno P (2009) Autophagy: regulation and role in disease. Crit Rev Clin Lab Sci 46:210–240

Michelakis ED, Webster L, Mackey JR (2008) Dichloroacetate (DCA) as a potential metabolic-targeting therapy for cancer. Br J Canc 99:989–994

Michelakis ED, Sutendra G, Dromparis P, Webster L, Haromy A, Niven E, Maguire C, Gammer T-L, Mackey JR, Fulton D, Abdulkarim B, McMurtry MS, Petruk KC (2010) Metabolic modulation of glioblastoma with dichloroacetate. Sci Transl Med 2:31ra34

Miller DM, Buettner GR, Aust SD (1990) Transition metals as catalysts of " autoxidation" reactions. Free Radic Biol Med 8:95–108

Miller EW, Dickinson BC, Chang CJ (2010) Aquaporin-3 mediates hydrogen peroxide uptake to regulate downstream intracellular signaling. Proc Natl Acad Sci (USA) 107:15681–15686

Mitchell PD (2004) Foundations of vectorial metabolism and osmochemistry. Biosci Rep 24:386–434

Mole DR, Blancher C, Copley RR, Pollard PJ, Gleadle JM, Ragoussis J, Ratcliffe PJ (2009) Genome-wide association of hypoxia-inducible factor (HIF)-1α and HIF-2α DNA binding with expression profiling of hypoxia-inducible transcripts. J Biol Chem 284:16767–16775

Morgan DJ, Sazanov LA (2008) Three-dimensional structure of respiratory complex I from *Escherichia coli* in ice in the presence of nucleotides. Biochim Biophys Acta 1777:711–718

Muller FL, Lustgarten MS, Jang Y, Richardson A, Van Remmen H (2007) Trends in oxidative aging theorie. Free Radic Biol Med 43:477–503

Murai M, Ishihara A, Nishioka T, Yagi T, Miyoshi H (2007) The ND1 subunit constructs the inhibitor binding domain in bovine heart mitochondrial complex I. Biochemistry 46:6409–6416

Murphy MP (2009) How mitochondria produce reactive oxygen species. Biochem J 417:1–13

Murphy MP, Holmgren A, Larsson N-G, Halliwell B, Chang CJ, Kalyanaraman B, Rhee SG, Thornalley PJ, Partridge L, Gems D, Nyström T, Belousov V, Schumacker PT, Winterbourn CC (2011) Unraveling the biological roles of reactive oxygen species. Cell Metab 13:361–366

Nakashima Y, Shinzawa-Itoh K, Watanabe K, Naoki K, Hano N, Yoshikawa S (2002) Steady-state kinetics of NADH:coenzyme Q oxidoreductase isolated from bovine heart mitochondria. J Bioenerg Bioemembr 34:11–19

Nulton-Persson AC, Szweda LI (2001) Modulation of mitochondrial function by hydrogen peroxide. J Biol Chem 267:23357–23361

Ohnishi ST, Shinzawa-Itoh K, Ohta K, Yoshikawa S, Ohnishi T (2010) New insights into the superoxide generation sites in bovine heart NADH-ubiquinone oxidoreductase (Complex I): the significance of protein-associated ubiquinone and the dynamic shifting of generation sites between semiflavin and semiquinone radicals. Biochim Biophys Acta 1797:1901–1909

Ohnishi T, Leigh JS, Ragan CI, Racker E (1974) Low temperature electron paramagnetic resonance studies on iron-sulfur centers in cardiac NADH dehydrogenase. Biochem Biophys Res Commun 56:775–782

Ohnishi T, Blum H, Galante YM, Hatefi Y (1981) Iron-sulfur N-1 clusters studied in NADH-ubiquinone oxidoreductase and in soluble NADH dehydrogenase. J Biol Chem 256:9216–9220

Okado-Matsumoto A, Fridovich I (2001) Subcellular distribution of superoxide dismutases (SOD) in rat liver: Cu, Zn-SOD in mitochondria. J Biol Chem 276:38388–38393

Orme-Johnson NR, Hansen RE, Beinert H (1974) Electron paramagnetic resonance-detectable electron acceptors in beef heart mitochondria. Reduced diphosphopyridine nucleotide ubiquinone reductase segment of the electron transfer system. J Biol Chem 249:1922–1927

Paech C, Reynolds JR, Singer TP, Holm RH (1981) Structural identification of the iron-sulfur clusters of the respiratory chain-linked NADH dehydrogenase. J Biol Chem 256:3167–3170

Papa S (1969) In: Papa S, Tager JM, Quagliariello E, Slater EC (eds) The energy level and metabolic control in mitochondria: control of the utilization of mitochondrial reducing equivalents. Adriatica Editrice, Bari, Italy, pp 402–409

Papandreou I, Goliasova T, Denko NC (2010) Anticancer drugs that target metabolism: is dichloroacetate the new paradigm? Int J Cancer 128:1001–1008

Parker N, Vidal-Puig AJ, Azzu V, Brand MD (2009) Dysregulation of glucose homeostasis in nicotinamide nucleotide transhydrogenase knockout mice is independent of uncoupling protein 2. Biochim Biophys Acta 1787:1451–1457

Parsons DW, Jones S, Zhang X, Lin JC-H, Leary RJ, Angenendt P, Mankoo P, Carter H, Siu I-M, Gallia GL, Olivi A, McLendon R, Rasheed BA, Keir S, Nikolskaya T, Nikolsky Y, Busam DA, Tekleab H, Diaz LA Jr, Hartigan J, Smith DR, Strausberg RL, Marie SKN, Shinjo SMO, Yan H, Riggins GJ, Bigner DD, Karchin R, Papadopoulos N, Parmigiani G, Vogelstein B, Velculescu VE, Kinzler KW (2008) An integrated genomic analysis of human glioblastoma multiforme. Science 321:1807–1812

Pastorino JG, Hoek JB (2008) Regulation of hexokinase binding to VDAC. J Bioenerg Biomembr 40:171–182

Pedersen A, Karlsson GB, Rydström J (2008) Proton-translocating transhydrogenase: an update of unsolved and controversial issues. J Bioenerg Biomembr 40:463–473

Pedersen A, Karlsson J, Althage M, Rydström J (2003) Properties of the apo-form of the NADP(H)-binding domain III of proton-pumping *Escherichia coli* transhydrogenase: implications for the reaction mechanism of the intact enzyme. Biochim Biophys Acta 1604:55–59

Pedersen PL (1978) Tumor mitochondria and the bioenergetics of cancer cells. Progr Exp Tumor Res 22:190–274

Peng G, Fritzsch G, Zickermann V, Schagger H, Mentele R, Lottspeich F, Bostina M, Radermacher M, Huber R, Stetter KO, Michel H (2003) Isolation, characterization and electron microscopic single particle analysis of the NADH:ubiquinone oxidoreductase (complex I) from the hyperthermophilic eubacterium *Aquifex aeolicus*. Biochemistry 42:3032–3039

Persson B, Enander K, Tang H-L, Rydstrom J (1984) Energy-linked nicotinamide nucleotide transhydrogenase. Properties of proton-translocating mitochondrial transhydrogenase from beef heart purified by fast protein liquid chromatography. J Biol Chem 259:8626–8632

Pollard PJ, Ratcliffe PJ (2009) Puzzling patterns of predisposition. Science 324:192–194

Pryde KR, Hirst J (2011) Superoxide is produced by the reduced flavin in mtiochondrial complex I: a single, unified mechanism that applies during both forward and reverse electron transfer. J Biol Chem 286:18056–18065

Ragan CI (1976) The effects of proteolytic digestion by trypsin on the structure and catalytic properties of reduced nicotinamide-adenine dinucleotide dehydrogenase from bovine heart mitochondria. Biochem J 156:367–374

Ragan CI, Racker E (1973) Resolution and reconstitution of the mitochondrial electron transport system. IV. The reconstitution of rotenone-sensitive reduced nicotinamide adenine dinucleotide-ubiquinone reductase from reduced nicotinamide adenine dinucleotide dehydrogenase and phospholipids. J Biol Chem 248:6876–6884

Ragan CI, Widger WR (1975) The reconstitution of the mitochondrial energy-linked transhydrogenase. Biochem Biophys Res Commun 62:744–749

Ringler RL, Minakami S, Singer TP (1960) Isolation and properties of the DPNH dehydrogenase of the respiratory chain from heart mitochondria. Biochem Biophys Res Commun 3:417–422

Ringler RL, Minakami S, Singer TP (1963) Studies on the respiratory chain-linked NADH dehydrogenase. II. Isolation and molecular properties of the enzyme from beef heart. J Biol Chem 238:801–810

Robinson JM, Smith MG, Gibbs M (1980) Influence of hydrogen peroxide upon carbon dioxide photoassimilation in the spinach chloroplast. I. Hydrogen peroxide generated by broken chloroplasts in an "intact" chloroplast preparation is a causal agent of the Warburg effect. Plant Physiol 65:755–759

Rossi C, Cremona T, Machinist JM, Singer TP (1965) Studies on the respiratory chain-linked reduced nicotinamide adenine dinucleotide dehydrogenase. VIII. Inactivation, fragmentation, and protection by substrates. J Biol Chem 240:2634–2643

Rydström J (1972) Site-specific inhibitors of mitochondrial nicotinamide-nucleotide transhydrogenase. Eur J Biochem 31:496–504

Rydström J (1977) Energy-linked nicotinamide nucleotide transhydrogenases. Biochim Biophys Acta 463:155–184

Rydström J (2006a) Mitochondrial transhydrogenase—a key enzyme in insulin secretion and, potentially, diabetes. Trends Biochem Sci 31:355–358

Rydström J (2006b) Mitochondrial NADPH, transhydrogenase and disease. Biochim Biophys Acta 1757:721–726

Rydström J, Montelius J, Bäckström D, Ernster L (1978) The mechanism of oxidation of reduced nicotinamide dinucleotide phosphate by submitochondrial particles from beef heart. Biochim Biophys Acta 501:370–380

Salerno JC, Ohnishi T, Lim J, Widger WR, King TE (1977) Spin coupling between electron carriers in the dehydrogenase segments of the respiratory chain. Biochem Biophys Res Commun 75:618–624

Sazanov LA, Hinchliffe P (2006) Structure of the hydrophilic domain of respiratory Complex I from *Thermus thermophilus*. Science 311:1430–1436

Scherz-Shouval R, Shvets E, Fass E, Shorer H, Gil L, Elazar Z (2007) Reactive oxygen species are essential for autophagy and specifically regulate the activity of Atg4. EMBO J 26:1749–1760

Semenza GL (2008a) Mitochondrial autophagy. Autophagy 4:534–536

Semenza GL (2008b) Regulation of oxygen homeostasis by hypoxia-inducible factor 1. Physiology 24:97–106

Sharpley MS, Shannon RJ, Draghi F, Hirst J (2006) Interactions between phospholipids and NADH:ubiquinone oxidoreductase (complex I) from bovine mitochondria. Biochemistry 45:241–248

Shinzawa-Itoh K, Seiyama J, Terada H, Nakatsubo R, Naoki K, Nakashima Y, Yoshikawa S (2010) Bovine heart NADH-ubiquinone oxidoreductase contains one molecule of ubiquinone with ten isoprene units as one of the cofactors. Biochemistry 49:487–492

Sinegina L, Wikström M, Verkhovsky MI, Verkhovskaya ML (2005) Activation of isolated NADH:ubiquinone reductase I (Complex I) from *Escherichia coli* by detergent and phospholipids. Recovery of ubiquinone reductase activity and changes in EPR signals of iron-sulfur clusters. Biochemistry 44:8500–8505

Sled VD, Rudnitzky NI, Hatefi Y, Ohnishi T (1994) Thermodynamic analysis of flavin in mitochondrial NADH: ubiquinone oxidoreductase (complex I). Biochemistry 33:10069–10075

Stratton MR, Campbell PJ, Futreal PA (2009) The cancer genome. Nature 458:719–724

Sun RC, Fadia M, Dahlstrom JE, Parish CR, Board PG, Blackburn AC (2010) Reversal of the glycolytic phenotype by dichloroacetate inhibits metastatic breast cancer cell growth in vitro and in vivo. Breast Cancer Res Treat 120:253–260

Suslick KS (1990) Sonochemistry. Science 247:1439–1445

Suslick KS, Flannigan DJ (2008) Inside a collapsing bubble: sonoluminescence and the conditions during cavitation. Annu Rev Phys Chem 59:659–683

Taylor SI, Mukherjee C, Jungas RL (1975) Regulation of pyruvate dehydrogenase in isolated rat liver mitochondria. Effects of octanoate, oxidation-reduction state, and adenosine triphosphate to adenosine diphosphate ratio. J Biol Chem 250:2028–2035

Terman A, Kurz T, Navratil M, Arriaga EA, Brunk UT (2010) Mitochondrial turnover and aging of long-lived postmitotic cells. The mitochondrial-lysosomal axis theory of aging. Antioxid Redox Signal 12:503–535

Tocilescu MA, Fendel U, Zwicker K, Kerscher S, Brandt U (2007) Exploring the ubiquinone binding cavity of respiratory complex I. J Biol Chem 282:29514–29520

Tocilescu MA, Fendel U, Zwicker K, Dröse S, Kerscher S, Brandt U (2010) The role of a conserved tyrosine in the 49-kDa subunit of complex I for ubiquinone binding and reduction. Biochim Biophys Acta 1797:625–632

Toye AA, Lippiat JD, Proks P, Shimomura K, Bentley L, Hugill A, Mijat V, Goldsworthy M, Moir L, Haynes A, Quarterman J, Freeman HC, Ashcroft FM, Cox RD (2005) A genetic and physiological study of impaired glucose homeostasis control in C57BL/6J mice. Diabetologia 48:675–686

Van Belzen R, Albracht SPJ (1989) The pathway of electron transfer in NADH: Q oxidoreductase. Biochim Biophys Acta 974:311–320

Van Belzen R, Van Gaalen MC, Cuypers PA, Albracht SPJ (1990) New evidence for the dimeric nature of NADH: Q oxidoreductase in bovine-heart submitochondrial particles. Biochim Biophys Acta 1017:152–159

Van den Broeke C, Radu M, Chernoff J, Favoreel HW (2010) An emerging role for p21-activated kinases (Paks) in viral infections. Trends Cell Biol 20:160–169

Van der Linden E, Faber BW, Bleijlevens B, Burgdorf T, Bernhard M, Friedrich B, Albracht SPJ (2004) Selective release and function of one of the two FMN groups in the cytoplasmic NAD^+-reducing [NiFe]-hydrogenase from *Ralstonia eutropha*. Eur J Biochem 271:801–808

Van der Linden E, Burgdorf T, De Lacey AL, Buhrke T, Scholte M, Fernandez VM, Friedrich B, Albracht SPJ (2006) An improved purification procedure for the soluble [NiFe]-hydrogenase of *Ralstonia eutropha*: new insights into its (in)stability and spectroscopic properties. J Biol Inorg Chem 11:247–260

Vásquez-Vivar J, Kalyanaraman B, Kennedy MC (2000) Mitochondrial aconitase is a source of hydroxyl radical—An electron spin resonance investigation. J Biol Chem 275:14064–14069

Vincent KA, Parkin A, Lenz O, Albracht SPJ, Fontecilla-Camps JC, Cammack R, Friedrich B, Armstrong FA (2005) Electrochemical definitions of O_2 sensitivity and oxidative inactivation in hydrogenases. J Am Chem Soc 127:18179–18189

Vissers MCM, Wilkie RP (2007) Ascorbate deficiency results in impaired neutrophil apoptosis and clearance and is associated with up-regulation of hypoxia-inducible factor 1α. J Leukoc Biol 81:1236–1244

Vissers MCM, Gunningham SP, Morrison MJ, Dachs GU, Currie MJ (2007) Modulation of hypoxia-inducible factor-1 alpha in cultured primary cells by intracellular ascorbate. Free Radic Biol Med 42:765–772

Volbeda A, Garcia E, Piras C, De Lacey AL, Fernandez VM, Hatchikian EC, Frey M, Fontecilla-Camps JC (1996) Structure of the [NiFe] hydrogenase active site: evidence for biologically uncommon Fe ligands. J Am Chem Soc 118:12989–12996

Volbeda A, Martin L, Cavazza C, Matho M, Faber BW, Roseboom W, Albracht SPJ, Garcin E, Rousset M, Fontecilla-Camps JC (2005) Structural differences between the ready and unready oxidized states of [NiFe] hydrogenases. J Biol Inorg Chem 10:239–249

Walker JE (1992) The NADH: ubiquinone oxidoreductase (complex I) of respiratory chains. Q Rev Biophys 25:253–324

Warburg O (1927) Über den heutigen stand des carcinomproblems. Naturwissenschaften 15:1–4

Warburg O (1948) Schwermetalle als Wirkungsgruppen von Fermenten, Verlag Dr. W. Saenger, 2. Auflage, Berlin

Warburg O (1954) Krebsforschung. Naturwissenschaften 41:485–486

Warburg O, Krippahl G (1960) Glykolsäurebildung in *Chlorella*. Z Naturforsch 15b:197–199

Warburg O, Posener K, Negelein E (1924) Über den stoffwechsel der carcinomzelle. Biochem Z 152:309–344

Watt W, Tulinsky A, Swenson RP, Watenpaugh KD (1991) Comparison of the crystal structures of a flavodoxin in its three oxidation states at cryogenic temperatures. J Mol Biol 218:195–208

Westermann B (2010) Mitochondrial fusion and fission in cell life and death. Nat Rev Mol Cell Biol 11:872–884

Whitehouse S, Cooper RH, Randle PJ (1974) Mechanism of activation of pyruvate dehydrogenase by dichloroacetate and other halogenated carboxylic acids. Biochem J 141:761–774

Wikström M (1984) Two protons are pumped from the mitochondrial matrix per electron transferred between NADH and ubiquinone. FEBS Lett 169:300–304

Wong JYY, Huggins GS, Debidda M, Munshi NC, De Vivo I (2008) Dichloroacetate induces apoptosis in endometrial cancer cells. Gynecol Oncol 109:394–402

Yagi T (1987) Inhibition of NADH-ubiquinone reductase activity by N, N'- dicyclohexylcarbodiimide and correlation of this inhibition with the occurrence of energy-coupling site 1 in various organisms. Biochemistry 26:2822–2828

Yamamoto N, Ushijima N, Koga Y (2009) Immunotherapy of HIV-infected patients with Gc protein-derived macrophage activating factor (GcMAF). J Med Virol 81:16–26

Yamamoto N, Suyama H, Nakazato H, Yamamoto N, Koga Y (2008) Immunotherapy of metastatic colorectal cancer with vitamin D-binding protein-derived macrophage-activating factor, GcMAF. Canc Immunol Immunother 57:1007–1016

Yip C, Harbour ME, Jayawardena K, Fearnley IM, Sazanov LA (2011) Evolution of respiratory complex I. "Supernumerary" subunits are present in the α-proteobacterial enzyme. J Biol Chem 286:5023–5033

Zhang H, Bosch-Marce M, Shimoda LA, Tan YS, Baek JH, Wesley JB, Gonzalez FJ, Semenza GL (2008) Mitochondrial autophagy is an HIF-1-dependent adaptive metabolic response to hypoxia. J Biol Chem 283:10892–10903

Zhang Y, Marcillat O, Giulivi C, Ernster L, Davies KJA (1990) The oxidative inactivation of mitochondrial electron transport chain components and ATPase. J Biol Chem 265:16330–16336

Zickermann V, Kerscher S, Zwicker K, Tocilescu MA, Radermacher M, Brandt U (2009) Architecture of complex I and its implications for electron transfer and proton pumping. Biochim Biophys Acta 1787:574–583

Zwicker K, Galkin A, Dröse S, Grgic L, Kerscher S, Brandt U (2006) The redox-Bohr group associated with iron-sulfur cluster N2 of complex I. J Biol Chem 281:23013–23017